JOURNAL OF GEOPHYSICAL RESEARCH, VOL. 104, NO. D17, PAGES 21,649–21,671, SEPTEMBER 20, 1999

Oceanographic context of the First Aerosol Characterization Experiment (ACE 1): A physical, chemical, and biological overview

F. B. Griffiths
CSIRO Marine Research, Castray Esplanade, Hobart, Tasmania, Australia.

T. S. Bates and P. K. Quinn
Pacific Marine Environmental Laboratory (PMEL), NOAA, Seattle, Washington

L. A. Clementson and J. S. Parslow
CSIRO Marine Research, Castray Esplanade, Hobart, Tasmania, Australia.

Abstract. The First Aerosol Characterization Experiment (ACE 1) intensive experiment, conducted between November 14 and December 15, 1995, covered an oceanographically complex region, including the subtropical (ST), Subtropical Convergence Zone (STCZ), Subantarctic (SA), and polar water masses. Oceanographic and atmospheric sampling to identify the chemical and biological communities that might affect biologically produced, aerosol precursors in these water masses was carried out from the RV *Discoverer* and FRV *Southern Surveyor*. Sea surface temperature was not a good indicator of water mass during ACE 1. The physical structure east of 147.5°E was more complex than west of this longitude. Nutrient concentrations (nitrate, silicate) in the mixed layer increased, but ammonia concentrations decreased from ST to polar waters. Ammonia concentrations in surface waters exceeded >5 μM, and ammonia fluxes peaked at 12 μM m^{-2} d^{-1} in ST water near Cape Grim between November 27 and 30. Seawater dimethyl sulfide (DMS_{sw}) concentrations averaged 1.7 ± 1.1 nM with maximum values near 6 nM in ST waters. The flux of dimethyl sulfide to the atmosphere averaged 4.7 ± 5.0 μM m^{-2} d^{-1}, with peak fluxes (>40 μM m^{-2} d^{-1}) in SA water. DMS_{sw} increased significantly only in SA waters during the experiment. Surface chlorophyll-*a* concentrations measured from the FRV *Southern Surveyor* ranged between 0.3 and 0.6 mg m^{-3}. Surface chlorophyll-a concentrations along the *Discoverer* cruise track were similar, but 5 phytoplankton blooms (>1 mg m^{-3}) were found. Integrated column chlorophylls ranged from 29.4 mg m^{-2} in SA water to 53.2 mg m^{-2} in ST water. Modeled primary production rates were ranged between 409 mg carbon m^{-2} d^{-1} in the polar front to 3180 mg carbon m^{-2} d^{-1} in ST water near Cape Grim. Mixed layer phytoplankton growth rates, estimated from net primary production, were 0.31 d^{-1} in the SAF to 1.07 d^{-1} in STCZ water east of Tasmania. Grazing dilution experiments showed microzooplankton grazing and phytoplankton growth rates were tightly coupled, with net growth rates ranging from -0.13 d^{-1} to 0.22 d^{-1}. During the ACE 1 intensive period, the surface waters were in transition from the deeply mixed, winter conditions to the shallowly stratified, spring conditions. The spring phytoplankton bloom was just beginning in the northern water masses, and isolated blooms were present at several locations in SA surface waters. The low standing stocks of chlorophyll and tightly coupled grazing rates may have been responsible for the low concentrations of DMS and NH_3 in the region, and the generally low fluxes of these compounds to the atmosphere during the ACE 1 intensive experiment.

1. Introduction

The oceanographic part of the First Aerosol Characterization Experiment (ACE 1) can be divided into a long transit from Seattle, Washington, to Hobart, Tasmania, conducted by the R/V *Discoverer* and the "ACE 1 intensive experiment" [*Bates et al.*, 1998a]. The ACE 1 intensive experiment took place in the area around and to the south of Tasmania between ~ 40°S and 58°S and 135°E and 157°E (Plate 1). This paper discusses only the ACE 1 intensive experiment, during which both the RV *Discoverer* and FRV *Southern Surveyor* were at sea, providing the oceanographic background to the concurrent atmospheric investigations.

The specific goal of ACE 1 were to determine and understand the properties and controlling factors of aerosols in the

Paper number 1999JD900386.
0148-0227/99/1999JD900386$09.00

remote marine environment that are relevant to radiative forcing and climate. The area west and south of Tasmania meets the requirements of a remote marine environment, particularly when west or southwest winds are blowing. Additional reasons for choosing the area are given by *Bates et al.* [1998a]. The objectives of this paper are to (1) describe the characteristics and locations of the near-surface water masses that were traversed during the ACE 1 Intensive experiment, (2) describe the nutrients (nitrate, silicate, phosphate, ammonia) in the water masses, and how these varied in time during the experiment, (3) describe the distribution of chlorophyll-*a* in both the surface water and with depth and column primary production, phytoplankton growth rates, and microzooplankton grazing rates, and (4) describe the water masses traversed and characterise the fluxes of DMS and ammonia from the ocean to the atmosphere, particularly during the Lagrangian experiments.

These objectives were designed to assess the role of the physical oceanographic structure, and mixed layer chemical and biological processes in controlling the rates at which biologically based aerosol precursors are produced.

In the ACE 1 region, water mass boundaries have previously been identified primarily based on the subsurface physical oceanographic structure, but this is not useful for work concentrating on mixed layer processes. Water masses are defined following *Rintoul et al.* [1997], *Jones et al.* [1998], and *Clementson et al.* [1998]. The mixed-layer, salinity front definitions approximately correspond to these subsurface temperature/depth combinations and are most useful for defining the water mass boundaries. Temperature could not be used as *Rintoul et al.* [1997] found significant warming and cooling in the mixed layer between October (late winter) and March (late summer) but little change in mixed layer salinity. Subtropical water has a surface salinity of >35.2, and the Subtropical Convergence Zone (STCZ) has salinities between 34.8 and 35.2. A salinity change at the surface to <34.8 approximates the position of the 11°C isotherm at 150 m. This salinity separated the Subtropical Convergence Zone water from the Subantarctic Zone (SAZ) and Subantarctic Front (SAF) which have a salinity range of 34.8–34.2. The Polar Front (PF) is adjacent to the SAF. A surface salinity of 34.0 approximates the 2°C temperature minimum layer at 200 m, defining the surface polar water mass in this paper.

Nitrate and silicate concentrations in the mixed layer of the ST water are generally <1 μM [*Clementson et al.*, 1998; *Jones et al.*, 1998]. Nitrate and silicate concentrations and increase in steps as the various water masses are encountered [*Maeda et al.*, 1985]. The STCZ, SA, and polar zones are high nitrate, low silicate low chlorophyll with low dissolved iron concentrations in the mixed layer regions [*Sedwick et al.*, 1997]. Chlorophyll-*a* concentrations in the mixed layer were in the 0.1-0.6 mg m^{-3} range and increased to >2 mg m^{-3} in phytoplankton blooms [*Bradford-Grieve et al.*, 1997]. Primary production in these waters can vary from <100 mg C $m^{-3} d^{-1}$ to >2000 mg $m^{-2} d^{-1}$ and is very dependent on season and region [*Harris et al.*, 1987, 1991; *Parslow et al.*, 1996; *Bradford-Grieve et al.*, 1997; *Clementson et al.*, 1998].

The ocean is the source of non-sea-salt sulfate found in the marine boundary layer. The sulfur is released from the ocean in the form of dimethyl sulfide (DMS). Phytoplankton species such as *Phaeocystis pouchetti, Emiliania huxleyi, Rhizosolenia setigera,* and *Gymnodinium* spp. are rich sources of the DMS precursor, dimethylsulphoniopropionate (DMSP) [*Keller et al.*, 1989; *Malin et al.*, 1993]. Blooms of *E. huxleyi* and *Phaeocystis* have been associated with high DMS concentrations [*Gibson et al.*, 1990; *Malin et al.*, 1993]. *Gymnodinium* spp was the only abundant, DMSP-rich species found during the ACE 1 intensive experiment [*Jones et al.*, 1998]. DMS in seawater can be produced from the conversion of DMSP in intact phytoplankton cells [*Stefels and van Boekel*, 1993] by the release of DMSP from cells during grazing by zooplankton [*Dacey and Wakeham*, 1986; *Leck et al.*, 1990] or during phases of stationary or declining growth [*Turner et al.*, 1988]. *Levasseur et al.* [1996] suggest that microzooplankton grazing and bacterial action play a dominant role in determining the timing and magnitude of DMS pulses following phytoplankton blooms. *Kiene and Bates* [1990] found that microbial DMS consumption was generally 10 times faster than the DMS flux to the atmosphere. However, microbial DMS consumption was similar in magnitude to air-sea exchange in the midlatitude North Pacific [*Bates et al.*, 1994].

Curran et al. [1998] have described the spatial and temporal variation in DMS and DMSP in seawater and air in the Australian sector of the Southern Ocean between 1991 and 1995. They found significant correlations between DMSP and chlorophyll-*a* on the World Ocean Circulation Experiment (WOCE) SR3 transect between Tasmania and Antarctica in January 1994 and on a second transect between 59°S and 67°S near 80°E. In January 1995, a significant correlation along SR3 was found only when chlorophyll-*a* levels less than 0.2ug l^{-1} were included. *Bates et al.* [1998b] and *De Bruyn et al.* [1998] have measured seawater and atmospheric DMS, and atmospheric sulfur dioxide concentrations and related these to processes controlling the distribution of particles in the lower marine boundary layer. *Jones et al.* [1998] have measured DMS and DMSP concentrations in relation to water mass, phytoplankton species abundance, and microzooplankton grazing during the ACE 1 intensive experiment. They did not find a significant correlation between chlorophyll-*a* and DMSP although the particulate DMSP: chlorophyll-*a* ratio increased with increased numbers of dinoflagellates.

The source of ammonia in the remote marine atmosphere is also from biological processes taking place in the mixed layer of the ocean. Ammonia concentration in the mixed layer is a balance between the regeneration rate resulting primarily from microheterotrophic grazers and bacteria [Harrison, 1992], phytoplankton utilisation, and flux to the overlying atmosphere. Fluxes of ammonia from the atmosphere to the ocean are thought to be extremely small. At the pH of seawater, about 90% of the ammonia are present as dissolved ammonium (NH_4^+), which is not directly involved in air-sea exchange.

By measuring the nutrient concentrations, primary production, and grazing rates, and knowing the phytoplankton species present in the mixed layer, it is possible to begin to understand some of the variability in different oceanographic regions and the overlying atmosphere.

2. Measurements

2.1. Cruise Tracks

The cruise tracks that the vessels followed are shown on Plate 1, with the numbers indicating day of year (DOY) (where noon on February 1 equals DOY 32.5) and the posi-

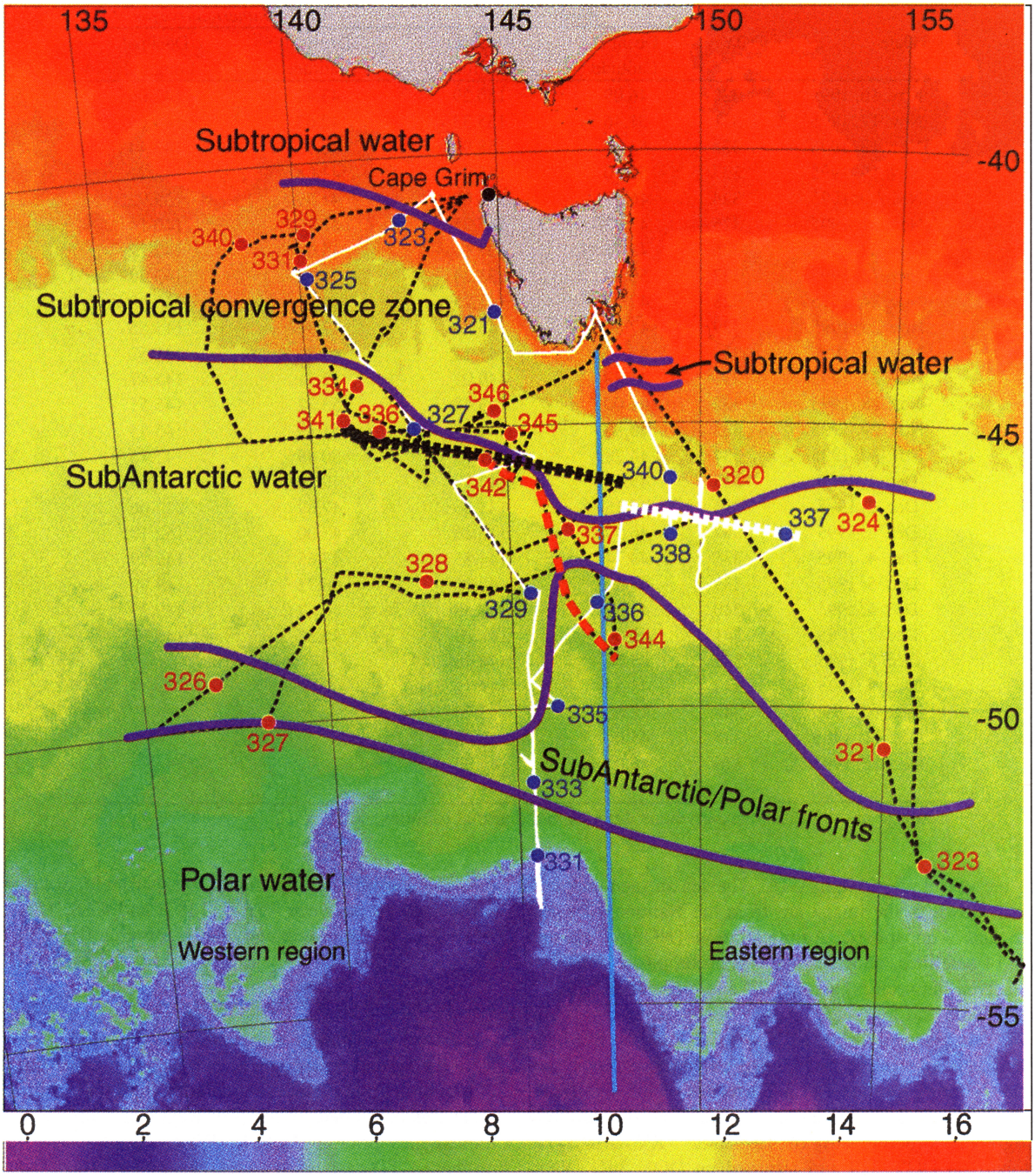

Plate 1. Composite sea surface temperature image for the period 24 November 24 to December 8, 1995, during the ACE 1 intensive experiment with the cruise tracks for the NOAA R/V *Discoverer* and FRV *Southern Surveyor* superimposed. The red circles and numbers represent *Discoverer*'s position at the beginning of each day of the year (DOY) at 0000 UTC, and the blue circles and numbers are the same for *Southern Surveyor*. The dotted black line represents *Discoverer*'s cruise track. The track made good by *Discoverer* during the Lagrangian A experiment is shown by the black rectangles and during the Lagrangian B by the red rectangles. The solid white line is *Southern Surveyor*'s cruise track, and the track made good during Lagrangian A is shown by the white rectangles. *Discoverer* left Hobart on November 15 (DOY 319) and returned on December 13, 1995 (DOY 347). *Southern Surveyor* left Hobart on November 16 (DOY 320) and returned on December 7, 1995 (DOY 341). The eastern and western regions are separated by a blue line along 147.5°E.

Table 1. Date, DOY, and Position of RV *Discoverer* and FRV *Southern Surveyor* at 0000 UTC During the ACE 1 Intensive Experiment

UTC Date	DOY	RV *Discoverer*		FRV *Southern Surveyor*	
		Decimal Latitude	Decimal Longitude	Decimal Latitude	Decimal Longitude
Nov. 16, 1995	320	46.09	150.29	43.41	147.06
Nov. 17, 1995	321	51.46	155.33	42.63	144.66
Nov. 18, 1995	322	54.51	158.97	40.73	143.44
Nov. 19, 1995	323	52.10	155.95	41.08	142.71
Nov. 20, 1995	324	46.23	154.03	41.99	139.92
Nov. 21, 1995	325	47.67	145.75	42.19	140.14
Nov. 22, 1995	326	48.95	137.61	45.00	142.72
Nov. 23, 1995	327	50.00	138.29	44.94	142.79
Nov. 24, 1995	328	47.52	141.25	46.31	143.88
Nov. 25, 1995	329	47.80	145.31	47.97	145.55
Nov. 26, 1995	330	43.32	141.15	48.81	145.52
Nov. 27, 1995	331	41.83	140.01	52.31	145.47
Nov. 28, 1995	332	41.00	143.48	53.32	145.51
Nov. 29, 1995	333	40.86	144.07	51.39	145.44
Nov. 30, 1995	334	44.28	141.15	50.49	145.45
Dec. 1, 1995	335	45.28	142.57	49.99	146.04
Dec. 2, 1995	336	45.15	141.53	47.89	147.66
Dec. 3, 1995	337	46.99	146.26	47.00	152.17
Dec. 4, 1995	338	44.74	141.53	47.65	149.99
Dec. 5, 1995	339	41.30	140.16	46.72	149.99
Dec. 6, 1995	340	41.30	138.58	46.57	149.23
Dec. 7, 1995	341	45.00	141.03	45.56	148.97
Dec. 8, 1995	342	45.54	144.48		
Dec. 9, 1995	343	45.57	144.36		
Dec. 10, 1995	344	48.60	147.70		
Dec. 11, 1995	345	45.06	145.05		
Dec. 12, 1995	346	45.01	144.00		

Latitude and longitude are given as degrees and decimal minutes.

tion of the vessel at midnight UTC. The sea surface temperature data shown in the image are from the National Oceanographic and Atmospheric Administration (NOAA) 12 and NOAA 14 satellites, and the image is a composite from images received between November 24 and December 8, 1995. Actual latitude and longitude of each vessel at 0000 UTC on each DOY is given in Table 1. The ACE 1 region has been separated into a "western block" and an "eastern block" approximately along latitude 147.5°E because of the significant influence of the East Australian Current on the physical oceanographic structure east of Tasmania. RV *Discoverer* left Hobart on DOY 319 and returned on DOY 346. Sampling near Macquarie Island (54°S, 159°E) was carried out between DOY 322-323. During the Lagrangian A experiment, *Discoverer* sampled between 45°S, 141°E and 46°S, 148°E on DOY 335-336, roughly under research flight 18 [*Bates et al.*, 1998a]. The region west and southwest of Cape Grim was sampled between DOY 330-341. Sampling to support the Lagrangian B experiment was done between 45.5°S, 144°E and 47°S, 146.1°E, and then south to 49.1°S, 147.7°E on DOY 342-343.

Southern Surveyor left Hobart on DOY 320, and returned on DOY 341. Work was concentrated along transects from Cape Grim to 42°S, 140°E, and between 42°S, 140°E and 53.2°S, 145.5°E (DOY 322-335), with additional intensive work in the region between 46°-47.5°S, 149°-150°E on DOY 337-340. During the Lagrangian A experiment, *Southern Surveyor* sampled between 46.5°S, 148°E and 47°S, 152.35°E on DOY 336-337, approximately under research flight 19.

2.2. Sampling on RV Discoverer

Vertical profiles of temperature and salinity were made from the surface to a depth of 300 m using a Seabird (SBE-9 Plus) conductivity/temperature/depth (CTD) instrument. The CTD was calibrated by the NW Regional Calibration facility immediately prior to ACE 1. Water samples were collected on these CTD casts with a rosette sampler using 10 L Niskin bottles with silicone O-rings and tubing. Eight CTD deployments were conducted from *Discoverer* during the ACE 1 intensive.

Discrete samples for chlorophyll-*a* measurements were collected every 4 hours while underway and at 10 depths from the CTD casts. Samples (530 mL) were collected, immediately filtered, and the filters were put into 10 mL of 90% acetone and stored in a freezer in the dark at -18°C. The samples were analyzed with a fluorometer aboard ship within 3-4 days of collection [*Parsons et al.*, 1984]. The fluorometer was calibrated after the cruise using standard chlorophyll-*a*.

2.2.1 Underway measurements. Seawater was sampled from the ship's clean seawater inlet at the bow of the NOAA R/V *Discoverer*, nominally 5 m below the sea surface [*Bates*

et al., 1998a]. Seawater temperature and salinity were measured with a Seabird SBE-21 thermosalinograph mounted in the clean seawater inlet in the ship's seachest at the bow of the ship. The thermosalinograph was calibrated by the Northwest Regional Calibration Centre immediately before the cruise. Temperatures were measured with an accuracy of 0.001°C, and salinity was measured in practical salinity units (psu) with an accuracy of 0.005. The data were stored as instantaneous 1-minute values. All salinities in this paper are reported using the Practical Salinity Scale 1978 (PSS 78), hence no units are included. Water from the seachest was pumped at a flow rate of 100 liters per minute (L min^{-1}) to the ship's laboratory for nitrate, ammonium, and DMS analysis.

The total nitrate and nitrite concentration was determined by standard autoanalyzer techniques [*Parsons et al.,* 1984]. At 10-minute intervals, the instrument sampled seawater, blank, seawater, blank, standard, blank, and this sequence was repeated each hour. The lower limit of detection ranged from 0.02 to 0.05 μM. Seawater from the ocean gyres was used both as the instrument blank and to prepare standards.

2.2.2 Seawater and atmospheric ammonia measurements. The total seawater ammonia concentration [$NH_4^+{}_{(s)}$+ $NH_{3(s)}$], shown as $[NHx]_{sw}$, was determined by the method of *Genfa and Dasgupta* [1989]. A continuous flow of seawater was injected into a manifold at regular intervals. In between each sample injection, a baseline was established by injecting blank seawater collected in the ocean gyres. NH_4^+ standards, made by standard addition to the gyre water also were periodically injected. The detection limit was 0.005 μM. The pH measurements were made in conjunction with the concentration [$NH_4^+{}_{(s)}$+ $NH_{3(s)}$] measurements in order to calculate $NH_{3(s)}$ for the flux calculations. The pH was determined using the spectrophotometric technique of *Dickson* [1993], and the accuracy is estimated to be ±0.005.

Atmospheric ammonia samples ($[NH_3]_{atm}$) were collected on oxalic coated filters mounted at the top of the aerosol sampling mast [*Bates et al.,* 1998a] using a tandem sampling system [*Quinn and Bates,* 1989; *Quinn et al.,* 1990]. A cyclone separator removed large sea-salt particles. The cyclone was followed by a 47 mm Millipore Fluoropore filter for the collection of the remaining particles and 4 Whatman 41 paper filters in series coated with 0.01 M oxalic acid for the collection of NH_3(g). Samples were analyzed by ion chromatography [*Quinn et al.,* 1998]. All sample handling was carried out in an NH_3-free glove box. On average, the blank concentration was 18% of the sample concentration. Values reported here are in units of nM m^{-3} at standard temperature (25°C) and pressure (1013 mbar) such that 1 nM m^{-3} equals 24.5 ppt.

2.2.3. Seawater and atmospheric DMS measurements. Seawater DMS concentrations were determined with a purge and trap system. Approximately every 30 min, 5.1 mL of seawater was valved into a Teflon gas stripper. The sample was purged with hydrogen at 80 mL min^{-1} for 5 min. Water vapor in the purged seawater sample stream was removed by passing the flow through a - 25°C Teflon tube filled with silanized glass wool. DMS was then trapped in a - 25°C Teflon tube filled with Tenax. During the sample trapping period, 6.2 pmol of methylethyl sulfide was valved into the hydrogen stream as an internal standard. At the end of the sampling/purge period, the coolant was pushed away from the trap and the trap, and the trap was electrically heated. The trapped sample was desorbed onto a DB-1 mega-bore fused silica column where the sulfur compounds were separated isothermally at 50°C and quantified with a sulfur chemiluminescence detector. The system was calibrated using gravimetrically calibrated permeation tubes. The precision of the analysis was typically ±8%. The detection limit during ACE 1 was approximately 0.8 pM. The performance of the system was monitored regularly by running blanks and standards through the entire system. Values reported here have been corrected for recovery losses. System blanks were below detection limit. Data are reported here in units of n*M*.

Air samples (4 L min^{-1}) for DMS analysis were collected through a Teflon line which ran approximately 60 m from the top of the aerosol sampling mast [*Bates et al.,* 1998a] to the analytical system. One hundred mL min^{-1} of this air was pulled through a KI solution at the analytical system to eliminate oxidant interferences [*Cooper and Saltzman,* 1993]. The air sample volume ranged from 0.5 to 1.5 L depending on the DMS concentration. Air samples were analyzed using the same trap/detector system that was used for seawater DMS analysis. Values reported here have been corrected for recovery losses. System blanks were below detection limit. Atmospheric DMS concentrations (DMS_{atm}) are reported in parts per trillion (ppt).

2.2.4. Calculation of fluxes. For the ACE 1 data set, DMS fluxes were calculated for each seawater measurement, using

$$F = k_l (DMS)_{sw} \quad (1)$$

where k_l is the transfer coefficient and is based on the in situ wind speed and the wind speed transfer velocity relationships of *Liss and Merlivat* [1986].

The air/sea flux of ammonia was calculated for each atmospheric ammonia measurement using

$$F=k_g [K_h(NH_3)_s - (NH_3)_g] \quad (2)$$

where k_g is the transport coefficient. $(NH_3)_{sw}$ was calculated from the measured total seawater ammonia concentration [$NH_4^+{}_{(s)}$+ $NH_{3(s)}$]and measured pH. A transport coefficient of 3000 cm h^{-1} was used [*Liss and Slater,* 1974]. All equilibrium constants were corrected for temperature and the ionic strength of seawater [*Stumm and Morgan,* 1981; *Danckwerts,* 1970].

2.2.5. Additional measurements. Additional measurements made aboard the ship [*Bates et al.,* 1998a] included atmospheric temperature, pressure, and humidity, wind speed and direction, rainfall rates, solar radiation, and atmospheric radon [*Whittlestone and Zahorowski,* 1998]. Atmospheric vertical profiles of temperature, dew point temperature, and wind speed and direction from radiosondes were also made [*Bates et al.,* 1998a]. The "smart" balloons used to mark and trace the air parcels repeatedly sampled by the C-130 aircraft during the Lagrangian experiments [*Businger et al., 1999*] were released by the *Discoverer.* All references to time are reported here in UTC.

2.3. Sampling on FRV Southern Surveyor

Detailed physical, chemical, and biological measurements were made from the FRV *Southern Surveyor* between November 15 and December 7, 1995, during the ACE 1 intensive period. One hundred and five CTD casts to depths of between 100 m and 1000 m were made with a Neil Brown Mark 3B WOCE standard CTD and 12 bottle rosette. Samples

were taken from 10 L Niskin bottles on the rosette for salinity, oxygen, and nutrients. Prior to the cruise, the thermistor on the CTD was calibrated at the Calibration Facility of CSIRO Marine Research. The Calibration Facility is National Association of Testing Authorities (NATA) registered, and the results of the calibration are traceable to the ITS 90 temperature scale. Salinity data from the CTD were calibrated using results obtained from the analysis of in situ samples collected from Niskin bottles on the CTD rosette. Samples were collected during the upcast of the CTD, and the salinities were measured using an inductively coupled salinometer (YeoKal) standardized with International Association for Physical Science of the Ocean (IAPSO) standard seawater. Discrete measurements of dissolved oxygen were made by the Winkler method on samples collected from Niskin bottles. Oxygen profiles were made using an oxygen probe on the CTD. The oxygen sensor data were calibrated postcruise based on the bottle sampling results and an algorithm described by *Owens and Millard* [1985] with coefficients estimated by non linear least squares regression using the Levenberg-Marquardt method. Nutrients (NO_3, PO_4, SiO_4) were analysed using a Technicon AA2 autoanalyzer [*Airey and Sandars,* 1987]. The nitrate method was modified with an Imidazole buffer used instead of the Grasshoff buffer, and the cadmium granules in the reducing column were not coated with copper. Lower limits of detection were 0.2 μM, 0.05 μM, and 0.5 μM for nitrate+nitrite, phosphate, and silicate, respectively. Ammonia was measured using an improved flow injection analysis procedure [R. J. Watson *et al.*, manuscript in preparation, 1999] based on *Jones* [1991]. Detection limits of this improved method were 20 nM, and repeatability was <10 nM. DMS and DMSP were measured as described by *Jones et al.* [1998].

2.3.1. Underway measurements. The water inlet for underway salinity, temperature, fluorescence, and nutrient measurements was located at 5 m depth below the ship's water line, and travel time within the vessel was <1 min. Salinity and temperature were measured using a SeaBird thermosalinograph, which had a stated accuracy of ±0.001 psu and ±0.01°C. The salinity sensor was out of calibration by about 0.2 psu during this cruise. The underway salinity data have been corrected by regressing the salinity measured by the thermosalinograph against the salinity in the surface niskin bottle taken at 65 CTD stations during the cruise. No temperature correction was applied to the data presented here.

A WETStar fluorometer was used to measure fluorescence in the thermosalinograph outflow water, which was kept nearly constant at 1 L min^{-1}. The fluorometer had a measurement range of 0.03-3 mg m^{-3} and a sensitivity of 0.03 mg m^{-3} chlorophyll-*a*. The instrument was cleaned with methanol, and the zero was checked with Milli-Q water approximately daily during the cruise. Chlorophyll-*a* samples, used to calibrate the fluorometer, were taken at night from the fluorometer overflow, filtered through GF/F filters and immediately stored in liquid nitrogen until analyzed ashore by high-performance liquid chromatography (HPLC) as described below. The underway fluorescence data were converted to chlorophyll-*a* using the following regression: chlorophyll-*a* equal to 0.00127 x underway fluorescence - 0.0769 (r^2 = 0.702, n = 13, and p< .001).

Prior to DOY 336, the surface samples from CTD casts were used to give a surface distribution of nutrients along the cruise track. After DOY 336, samples for nutrient analysis were taken at approximately hourly intervals and frozen until analyzed as described above.

2.3.2. Primary production estimates. At the 19 sites, where primary production was measured (Table 2), profiles of downwelling irradiance (PAR) and in situ fluorescence were obtained using a LI-COR LI-192SB underwater 2π quantum sensor and a Sea-Tech fluorometer, respectively. Both instruments were mounted on the frame of the CTD. Primary production estimates and photosynthetic parameters were determined using a small-bottle ^{14}C technique modified from *Lewis and Smith* [1983] and described by *Mackey et al.* [1995]. Usually, six depths per station between the surface and 100 m were sampled using Niskin bottles fitted with silicon rubber O-rings and tubing. Water samples (4-6 L) for chlorophyll-*a* and pigment determinations were taken from the same niskin as the primary production samples. The samples for chlorophyll-*a* were filtered through Whatman 47 mm diameter, GF/F filters under low vacuum, and the filters were stored in liquid nitrogen until analyzed by HPLC. Chlorophyll-*a* and other pigments were initially extracted in 100% acetone with the final extract mixture being 90:10 acetone: water (vol: vol). The extracts were centrifuged and then filtered through a 0.2 μm membrane filter (Whatman, anatope) prior to analysis. The HPLC was a Waters high-performance liquid chromatograph, comprising a 600 controller, 717 plus refrigerated autosampler, and a 996 photo-diode array detector. Pigments were separated using a stainless steel 25 cm by 4.6 mm ID column packed with ODS2 of 5 μm particle size (SGE) with gradient elution as described by *Wright et al.* [1991]. The separated pigments were detected at 436 nm and identified against standard spectra using Waters Millennium software. Concentrations of chlorophyll-*a* in sample chromatograms were determined from calibration curves of prepared standards of chlorophyll-*a* (Sigma Chemicals). Fluorescence profiles with depth were converted to chlorophyll-*a* profiles using a regression between HPLC chlorophyll-*a* and fluorescence at the sampling depth on a cast by cast basis. The bottom of the mixed layer was defined as the first depth at which there was a change of 0.05°C, or 0.05 in salinity over a 10 m depth interval. After standardizing the primary production rates to chlorophyll-*a*, a non-linear parameter estimation routine was used to fit the P-I models of *Platt et al.* [1980] to the data following the procedures given by *Mackey et al.* [1995].

2.3.3. Production modeling. The gross, daily depth-integrated column production was calculated by integrating production at 1 m depth intervals from the surface to 110 m, and at 10 min time steps. A simple model incorporating the photosynthetic parameters (P_m^B, α, β), attenuation coefficients, chlorophyll-*a* profiles, and surface irradiance was used. Photosynthetic parameters were linearly extrapolated between sample depths. This model was generally the same as that described by *Mackey et al.* [1995] and integrated production over depth and time of day. Depth-integrated production was calculated in two ranges: from the surface to the bottom of the mixed layer, and from the bottom of the mixed layer to the maximum depth sampled (usually 110 m). We will refer to these estimates as modeled production.

Growth rates (μ, d^{-1}) from the modeled primary production results were calculated following *Parsons and Takahashi,* [1975]

$$\mu = 1/t \times \ln(C + \Delta C)/C \quad (3)$$

Table 2. Summary of Production and Grazing Dilution Results Done on *Southern Surveyor*

Latitude, °S	Longitude, °E	DOY	Water Mass	1% Light Depth	MLD	Chl-*a* in the Mixed Layer	Chl-*a* Below the Mixed Layer	Gross Production in Mixed Layer	Gross Production Below Mixed Layer	Total Column Production Mg Carbon m^{-2} d^{-1}	Specific Growth Rate in Mixed Layer	Specific Growth Rate Below Mixed Layer,	GD Growth Rates (NH_4 Added)	Grazing Rates	Net rate of population change
-40.8	143.4	322	ST	60	50	31.4	21.8	3045	142	3187	0.78	-0.30			
-42.0	140.0	324	ST	61	61	38.5	11.2	1711	25	1736	0.42	-0.09	0.47	0.40	0.07
-42.0	139.8	325	ST	63	52	31.2	13.4	2253	86	2339	0.69	-0.08			
-45.0	142.7	326	SA	67	9	2.4	34.0	182	930	1112	0.83	0.24	0.57	0.37	0.20
-45.0	142.8	327	SA	61	9	3.6	46.4	165	797	962	0.49	0.11			
-46.0	143.6	328	SA	68	8	2.5	31.8	91	684	776	0.65	0.35			
-48.0	145.5	329	SA	75	37	6.5	17.6	299	288	587	0.55	0.12	0.41	0.23	0.18
-48.0	145.7	330	SA	72	8	1.6	26.8	81	539	620	0.58	0.23			
-50.0	145.8	335	SAF	70	88	27.7	3.6	782	7	789	0.31	-0.07	0.52	0.30	0.22
-50.0	146.0	335	SAF	68	89	30.4	4.6	1164	14	1178	0.38	-0.09			
-51.0	145.4	334	PF	67	7	2.0	34.9	50	359	409	0.31	0.11			
-51.4	145.5	333	PF	74	51	11.2	14.2	327	119	446	0.35	0.03			
-53.3	145.5	331	P	63	36	12.2	32.2	325	211	536	0.34	0.01	0.64	0.77	-0.13
-53.3	145.5	332	P	71	42	9.0	20.8	594	233	828	0.69	0.04			
								Eastern Block							
-46.0	150.0	339	STCZ	66	41	19.8	19.6	1538	201	1740	0.75	-0.05			
-47.7	150.0	338	SA	78	35	5.4	14.4	544	435	978	0.96	0.27			
-48.0	150.0	338	SA	71	45	11.2	18.3	1134	284	1418	0.93	-0.07			
-46.6	149.2	340	STCZ	64	32	20.0	22.0	1547	384	1931	0.79	0.05	0.38	0.51	-0.13
-46.6	149.2	340	STCZ	63	22	14.6	28.6	1158	817	1975	1.07	0.24			

The table includes station position, water mass sampled, the 1% light depths, the mixed layer depths (MLD), chlorhyll- in and below the mixed layer (mg m^{-2}), gross primary production in and below the mixed layer, and total column primary production (mg carbon m^{-2} d^{-1}), phytoplankton specific growth rate (in $days^{-1}$ calculated from the net production in and below the mixed layer). Results from the grazing dilution experiments with the ammonia-enriched growth rate (d^{-1}), the microzooplankton grazing rates (d^{-1}), and the net rate of phytoplankton population change (d^{-1}) are also shown. The water mass abbreviations used are ST, subtropical; STCZ, Subtropical Convergence Zone; SA, Subantarctic; SAF, Subantarctic front; PF, polar front; and P, the polar water mass. See text for a definition of each zone.

with C being the standing stock of carbon converted from chlorophyll concentration and ΔC being the net, modeled production in and below the mixed layer, assuming a respiration rate of 10% [*Parsons and Takahashi,* 1975]. As we were working in a high nutrient-low chlorophyll (HNLC) region, a carbon to chlorophyll ratio of 50 [*Eppley,* 1972] was used to calculate growth rates.

There is still some uncertainty as to whether short-term ^{14}C P-I experiments measure net or gross photosynthesis [*Dring and Jewson,* 1982]. Given that our incubation period was short, and the production model does not allow for dark respiration, the modeled production results are probably closer to gross than net production. The error bounds on the integrated column production approach are difficult to develop, as they depend nonlinearly on multiple P versus I parameters. The standard error in modeled column production is estimated to be less than 30% and is fully discussed by *Clementson et al.* [1998].

2.3.4. Grazing dilution experiments. Grazing dilution experiments were carried out at six sites (Table 2) following the methods of *Landry and Hassett* [1983] and *Landry* [1993]. Water for these experiments was collected at 25 m depth with a Niskin bottle. Dilution water was prepared by filtering seawater through a 0.2 μm Supor filter into a carboy. Four dilutions (containing 100% unfiltered seawater (UFSW), 70% UFSW, 40% UFSW, and 10% UFSW) of phytoplankton and microzooplankton were prepared in 2 L polycarbonate bottles (three replicates per dilution) and spiked with 2 μ*M* ammonia. The bottles were incubated for 24 hours (±2 hours) in deck incubators at approximately 50% of surface light and at ambient sea surface temperature. Three randomly selected bottles were filtered at time zero, and the mean chlorophyll-*a* concentration in these bottles (determined by HPLC analysis) was used to calculate the initial chlorophyll-*a* concentration in each of the incubated bottles. At the conclusion of the experiment, the remaining bottles were filtered and analyzed for chlorophyll-*a* and pigments by HPLC. Grazing and growth coefficients were determined from a linear least squares regression analysis between the portion of undiluted water in each bottle, and the chlorophyll-*a* content of this water at the end of the incubation period [*Landry and Hassett,* 1983]. The specific growth rate of phytoplankton was calculated as the sum of the estimated grazing mortality and the net growth of phytoplankton without added nutrients. The time-averaged grazer density used in the calculation of grazing mortality [*Landry,* 1993) was estimated by preserving one 2 L sample at the start and finish of each experiment and counting the microzooplankton present.

2.3.5 Additional measurements. Additional atmospheric measurements made aboard *Southern Surveyor* included atmospheric temperature, pressure, and humidity, wind speed and direction, solar radiation, and atmospheric radon [*Whittlestone and Zahorowski,* 1998]. Atmospheric vertical profiles of temperature, dew point temperature, and wind speed and direction from radiosondes were also made [*Bates et al.,* 1998a]. *Jones et al.* [1998] have discussed DMS and DMSP distributions in relation to water mass and time, and *Curran et al.* [1998] showed there was no significant difference in DMS measured on the two vessels. Other seawater measurements made included fCO2, dissolved inorganic carbon, and alkalinity; and total organic and particulate carbon. Samples were collected for phytoplankton species identification and phytoplankton carbon biomass. These results will be reported separately.

3. Results

3.1. Discoverer/Southern Surveyor Intercomparisons

Discoverer and *Southern Surveyor* met at 48°S, 145.5°E on DOY 328 to do an intercalibration CTD and chlorophyll cast. The two ships did a simultaneous CTD cast to 1000 m and took samples for chlorophyll-*a* analyses. The temperature profiles (Figure 1a) are essentially identical, but the *Southern Surveyor* salinity results below the mixed layer are about 0.005 higher than on *Discoverer* (Figure 1b). Although a systematic difference in calibration between the two instruments cannot be ruled out, these differences are not significant when used to separate water masses. The two data sets have been combined to set the water mass limits in this paper. The chlorophyll-*a* profiles (Figure 2) from the two CTD casts show very similar trends, with the chlorophyll-*a* levels measured by fluorometry on *Discoverer* slightly higher than those measured by HPLC analysis on *Southern Surveyor. Mantoura et al.* [1997] compared fluorometric and HPLC methods of chlorophyll-*a* determination and found fluorometric methods can overestimate chlorophyll-*a*, especially where phaeopigments or degradation products were present in samples.

3.2. Water Mass Distribution During the ACE 1 Intensive Experiment

3.2.1. Surface water mass boundaries. The boundaries of the salinity-defined, surface water masses (Plate 1) were established by combining the thermosalinograph records from the Southern Surveyor (Figures 3a and 3b) and Discoverer (Figures 4b and 4c), and plotting the location of the surface salinity fronts. The small ribbon of warm, subtropical water seen in Plate 1 just southeast of Tasmania was a filament from the East Australian Current that was moving south just off the shelf break. The subtropical water seen near Cape Grim is the end of the Leeuwin Current extending from the Great Australian Bight [Godfrey et al., 1986]. The boundary between the STCZ and SA water sloped southeast between 137°E and 146°E, and then had a mainly east-west orientation between 146°E and 155°E. The surface temperatures along this boundary ranged between 11°C and 14°C. There is a large meander visible in the SAF/northern Polar Front between 145°E and 146°E, between 47°S and 51°S. Polar water temperatures ranged between 3°C and 10°C, while SA water temperatures ranged between 7°C and 13°C.

3.2.2. Subsurface water masses in the western region. The region has been divided into a western and eastern region along about 147.5°E because of the impact of the East Australian Current on the STCZ and SA water mass distributions [*Clementson et al.*, 1998]. The distribution of the principal subsurface water masses in the western region was determined from the CTD transect completed by *Southern Surveyor* between 42°S and 53.3°S between 140°E and 145.5°E (Figure 5). Although this transect is not along a single meridian, we are treating it as a direct north-south line in this paper. Subtropical Convergence Zone water was present between 42°S and about 44°S, and the Subantarctic water (between 44°S to about 50.2°S) formed the largest water mass

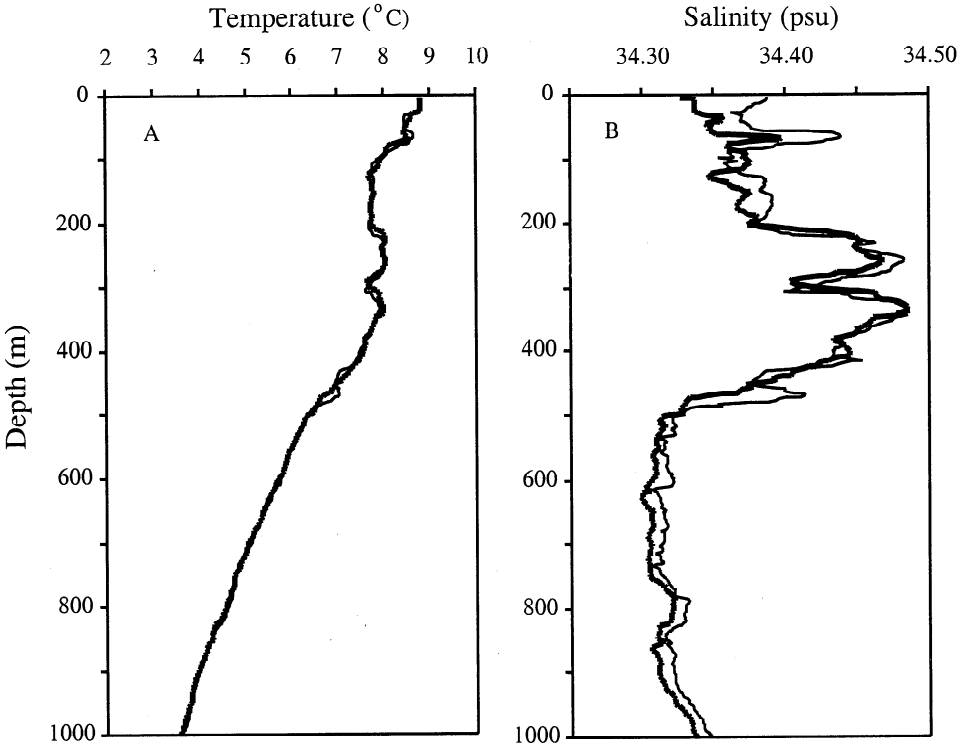

Figure 1. Comparison of (a) temperature and (b) salinity profiles from CTD casts at 48°S, 145.5°E made from *Discoverer* (station 20041, heavy line) and *Southern Surveyor* (station 43, light line) on November 24, 1995 (DOY 328). The CTD casts were made simultaneously, with the two ships about 0.5 nautical miles apart.

along the section. The Subantarctic Front, characterized by a rapid decrease in temperature (8°C to 3°C) and vertical isohalines and isotherms between the surface and at least 300 m, was crossed between 50.25°S and 50.75°S (Figures 5a and 5b). The northern edge of the Polar Frontal zone, characterised by salinities <34.2, was at approximately 51°S. Water characteristic of the polar water mass (surface salinities <34.2, and a temperature of <2°C in the 100–200 m depth range) was present at 53°S. The subsurface structure in the upper 1000 m along this transect was dominated by the Subantarctic Mode water [McCartney, 1977], seen as the broad thermostad of 8°-9°C water (Figure 5b) lying between depths of 100 and 650 m between 42°S and 49.5°S. This mode water is density-compensated by small changes in salinity and temperature in the thermostad, as evidenced from the widely spaced density contours (Figure 5c). There was a subsurface, cold-core eddy about 100 km in diameter centered near 48.5°S. This eddy is not visible in the sea surface temperature image (Plate 1). Surface currents, measured as drift of *Southern Surveyor* near the eddy, were about 20 cm s^{-1} eastward at 48°S, 31 cm s^{-1} westward at 49°S, and 56 cm s^{-1} eastward at 50°S. Advection of warmer, saltier water past the vessel during the station at 48°S caused the mixed layer to shallow from 37 m to 8 m.

3.2.3. Water mass boundaries in the eastern region: DOY 319-325. The eastern region was the area covered by research aircraft flights 16, 19, 20, 25, and 26 [*Bates et al.* 1998a]. Between DOY 319-321, RV *Discoverer* sailed from Hobart to Macquarie Island (Plate 1). A filament of subtropical water, identified by salinity >35.2, was crossed just off the southeast corner of Tasmania between 43.5°S, 147.8°E, and 43.6°S, 147.9°E. The track entered STCZ water near 44.4°S, 148.6°E, and surface nitrate increased from < 8μ*M* to >9 μ*M*. The ship crossed into the SA water mass at about 46.0°S, 150.2°E, and nitrate values increased to >10 μ*M*. The SAF was crossed between about 50.6°S, 154.9°E and 51.8°S, 155.4°E. Polar waters were entered at about 51.8°S, 155.5°E,

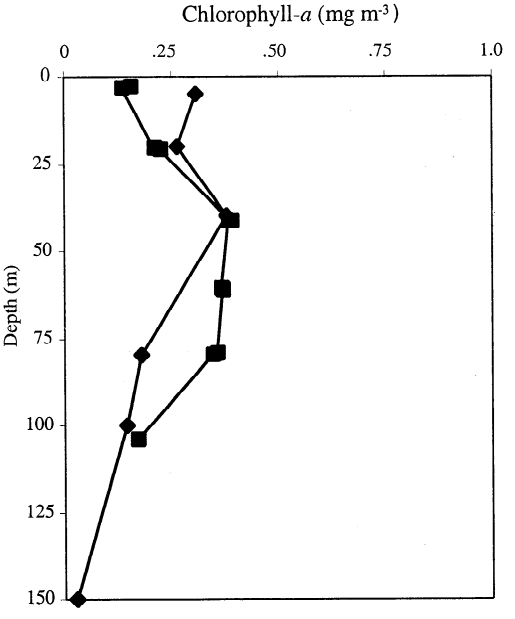

Figure 2. Comparison of chlorophyll profiles from extracted chlorophyll-*a* measured by fluorometry from *Discoverer* (station 20041, diamonds) and HPLC from *Southern Surveyor* (station 43, squares) on November 24, 1995 (DOY 328) from the simultaneous CTD cast at 48°S, 145.5°E.

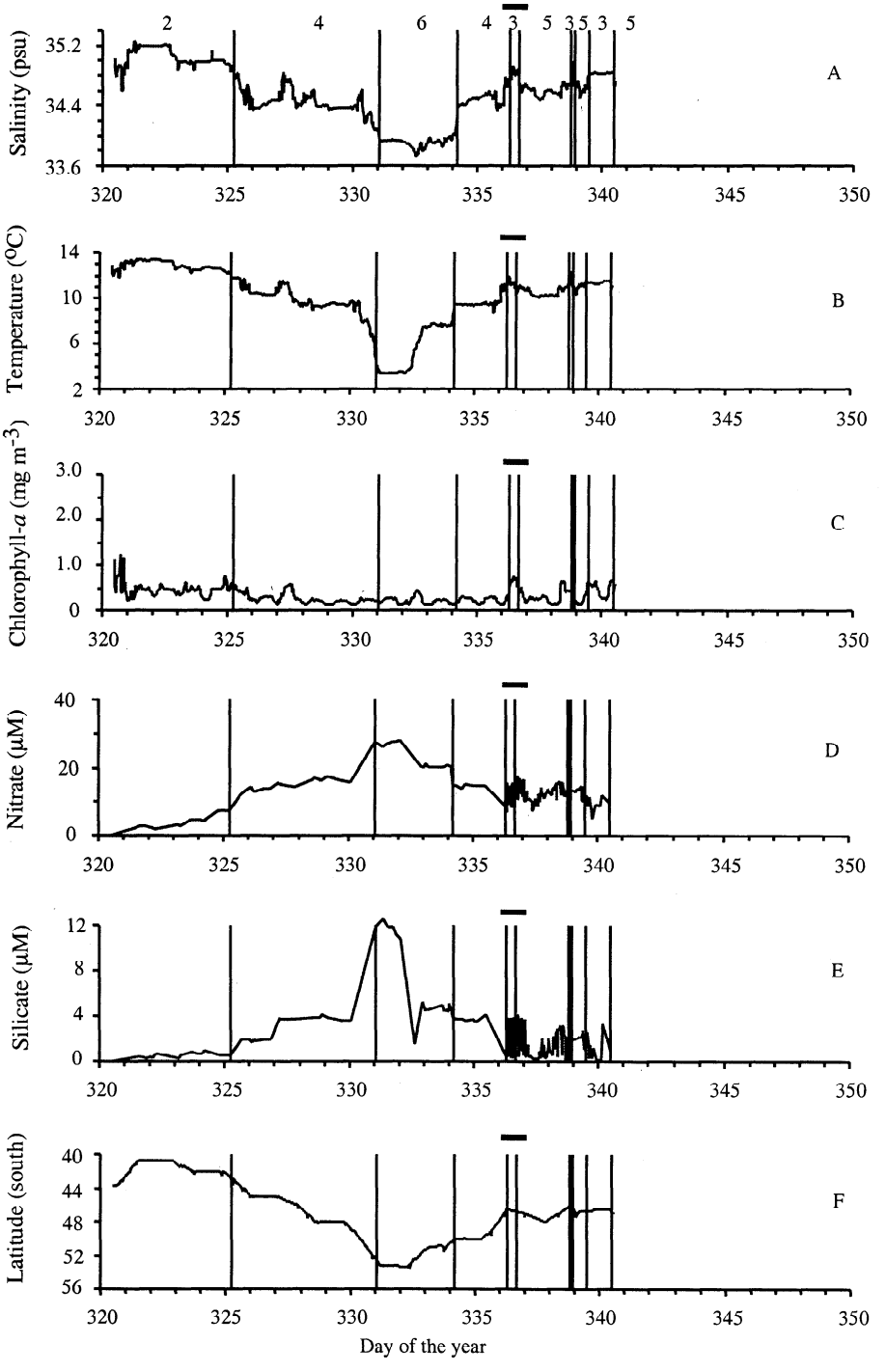

Figure 3. Sea surface (a) salinity (psu), (b) temperature (°C), (c) chlorophyll-*a* (mg m^{-3}), (d) nitrate (μ*M*), (e) silicate (μ*M*), and (f) latitude (degrees south) along the *Southern Surveyor* cruise track (Plate 1) plotted against DOY. The horizontal line between DOY 336 and 337 indicates sampling during the Lagrangian A experiment. The vertical lines show where the FRV *Southern Surveyor* crossed between water masses, and the numbers represent the water masses as follows: 1, subtropical; 2, western STCZ; 3, eastern STCZ; 4, western SA; 5, eastern SA; 6, western polar; 7, eastern polar.

where surface salinities fell to <34.0, and nitrate increased to about 16 μ*M*. Near Macquarie Island, surface salinities were <33.9, and surface nitrate was >20 μ*M* (Figures 4c and 4e), evidence that the vessel was approaching the northern edge of southern Polar Front. Frontal boundaries had not moved as *Discoverer* moved north DOY 323, and then turned west on DOY 324.

3.2.4. Water mass boundaries in the eastern region: DOY 337-340. Southern Surveyor sampled along a short north-south transect between 46°S and 47.4°S along 150°E between DOY 337 and 338, and at 46.2°S, 149.2°E on DOY 339. The boundary between the Subtropical Convergence Zone and Subantarctic water masses was about 47.2°S, 150°E, some 70 nautical miles farther south than where it was found

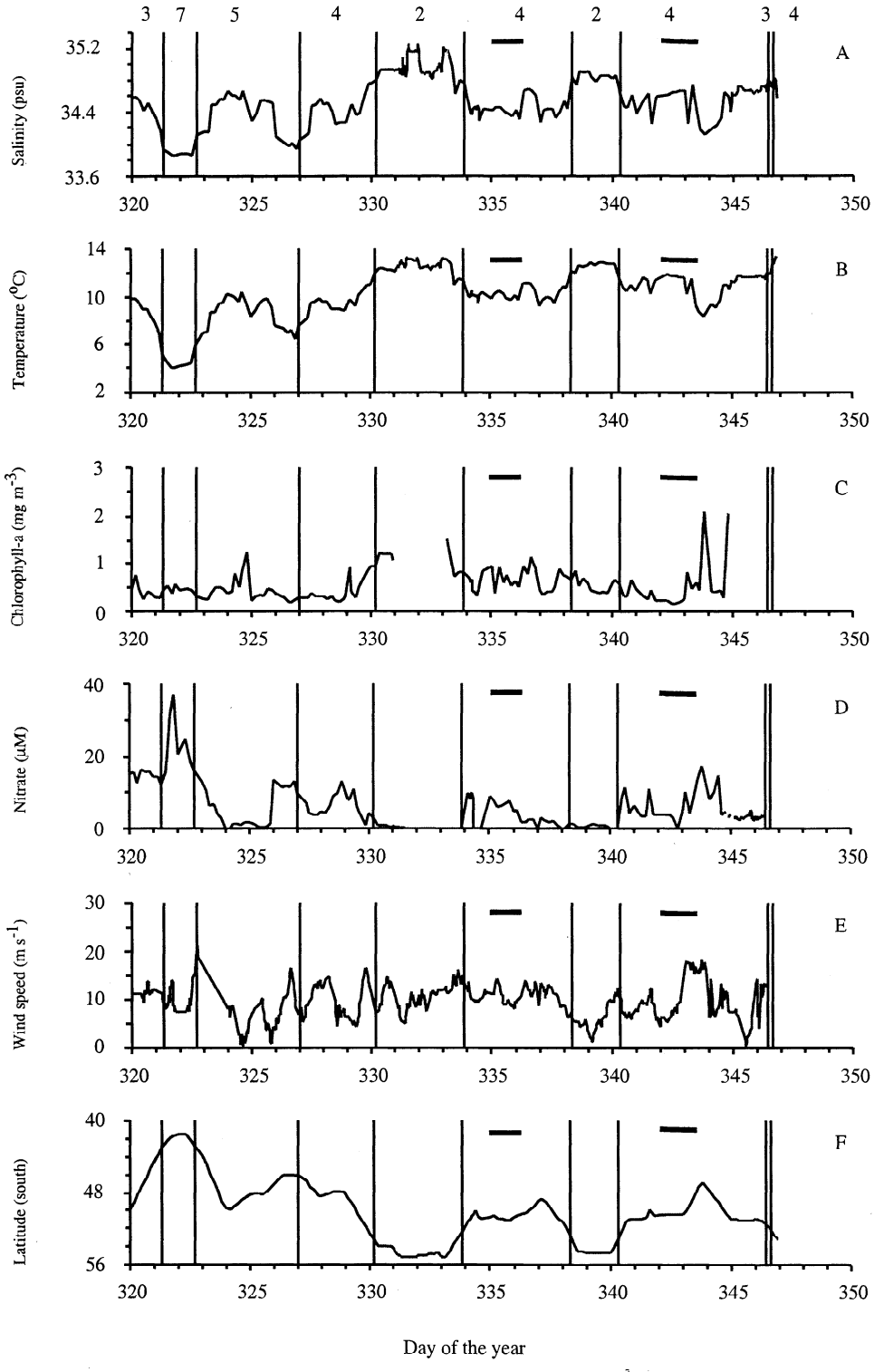

Figure 4. (a) Salinity (psu), (b) temperature (°C), (c) chlorophyll-*a* (mg m^{-3}), (d) nitrate (μM), (e) wind speed (m s^{-1}), (f) latitude (degrees south), (g) DMS_{sw} (nM), (h) DMS flux (μM m^{-2} d^{-1}), (i) DMS_{atm} (ppt), (j) $[NHx]_{sw}$ (μM), (k) NH_3 flux (μM m^{-2} d^{-1}), and (l) $[NH_3]_{atm}$ (nM m^{-3}) in surface waters south and west of Tasmania along the *Discoverer* cruise track (Plate 1) shown as a function of time. The horizontal lines between DOY 335-336 and DOY 343-344 mark sampling during the Lagrangian A and Lagrangian B experiments. The vertical lines show where the RV *Discoverer* crossed between water masses, with water masses identified as in Figure 3.

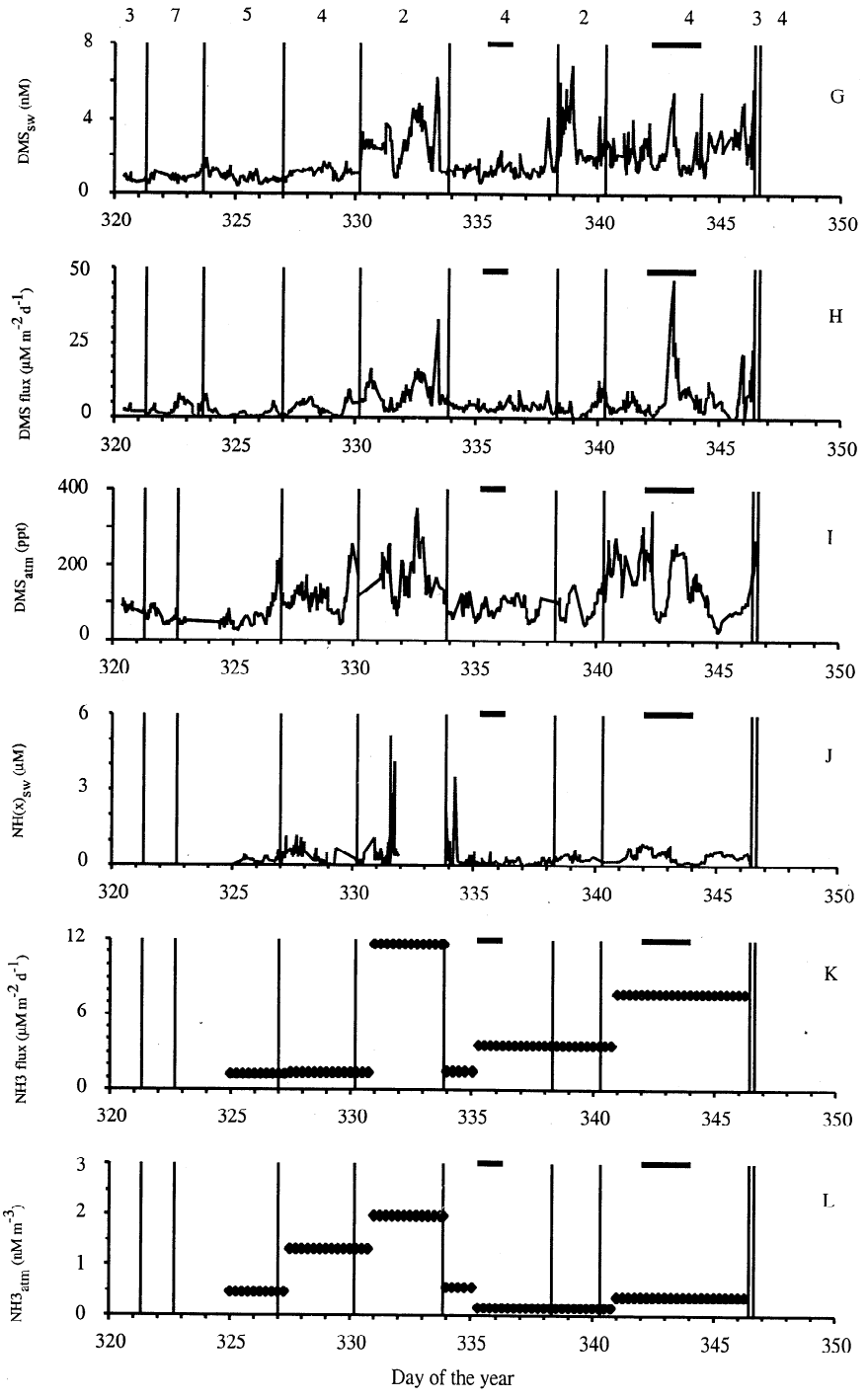

Figure 4. (continued)

on DOY 320 by Discoverer. This rapid movement of the front between DOY 320 and DOY 337 may be related to the movement of a meander visible on the SST image (Plate 1). Clementson et al. [1998] argued that the positions of the fronts south of Tasmania are strongly modulated by these mesoscale features at timescales ranging from days to years.

The vertical structure (Figure 6) in the upper 200 m shows the water mass distribution was much more complex than the surface data suggest. There was a <20 m deep lens of warm, salty, STCZ water (Figure 6b) that extended southward to 47.2°S over the underlying SA water. Below 25 m, the SA water extended north to about 46.4°S. A lens of STCZ water was seen between depths of 50 and 150 m in the SA water mass between latitudes of 46.8°S-47.2°S. The vertical temperature (Figure 6c) and density (Figure 6d) structures show the near-surface pycnocline was due to high-salinity water.

3.3. Underway Measurements During the ACE 1 Intensive Experiment

3.3.1. Distribution of nutrients and chlorophyll-a in surface waters. The distribution of nitrate (Figures 3d and

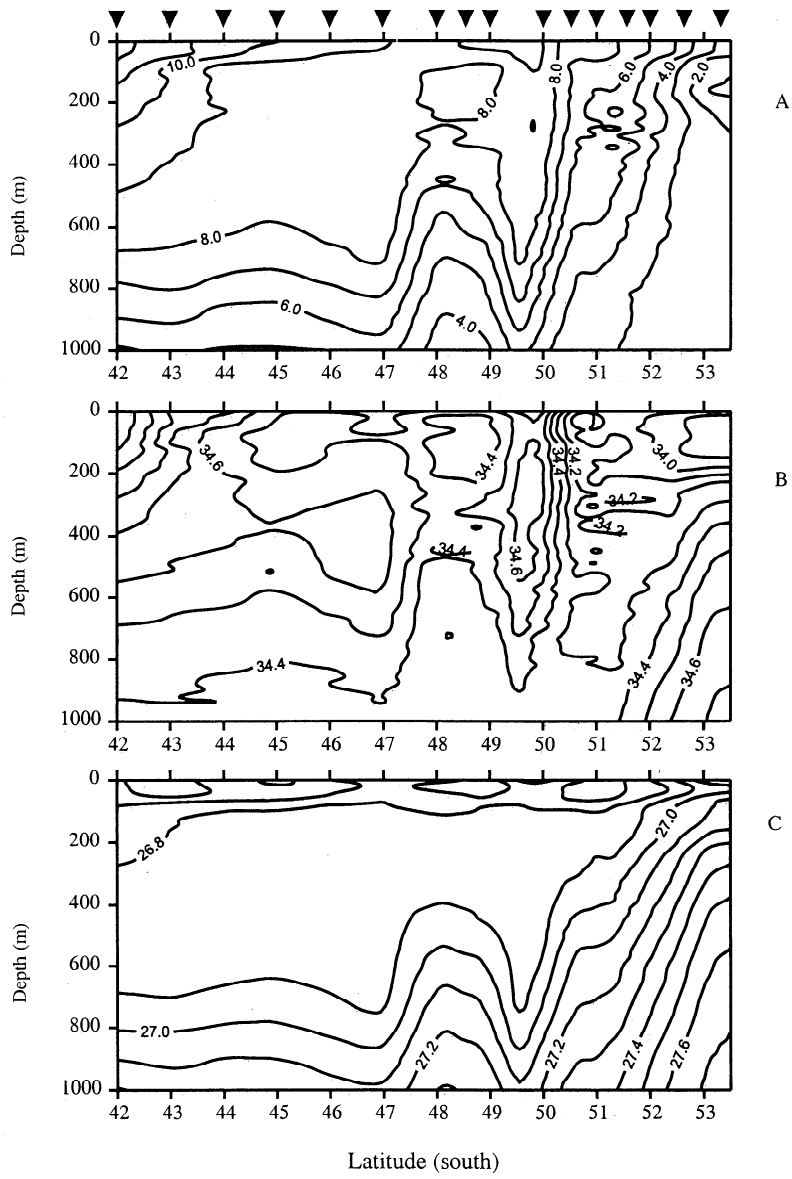

Figure 5. Contours of (a) temperature, (b) salinity, and (c) density between the surface and 1000 m along the western transect occupied by *Southern Surveyor* between 42°S, 140°E and 53.5°S, 145.5°E. The contour intervals are temperature, 1.0°C, salinity, 0.2 practical salinity units, and density 0.1 sigma-theta units. The positions of the CTD stations are indicated by a solid triangle. A low-salinity, cold-core eddy is visible between 48°S and 49°S in the upper 300 m. The SAF/PF is present between about 50°S and 52.5°S, and polar water can be seen south of 52.8°S. The large thermostad of 8°C water between 100 m and 650 m depth, and between latitudes of 44°S-47.5°S is mode water.

4c), silicate (Figure 3e), and phosphate (not shown) in surface waters reflects the vertical profiles in the underlying water. Nitrate concentrations measured on both vessels were similar and exhibited stepwise increases as the major fronts were crossed. Within water masses, increases of nitrate with latitude were seen in the SA and polar water masses. Nitrate and silicate values were somewhat higher in the eastern STCZ after DOY 336 than in the western STCZ (Figures 3d and 3e). Silicate concentrations in the STCZ region were low enough (<1 μM) to be limiting diatom growth.

The underway chlorophyll-*a* results along *Southern Surveyor's* cruise track were comparatively high (0.6-1.2 mg m^{-3}) and variable on the Tasmanian shelf and slope (to DOY 321). In STCZ waters they dropped to between 0.35 and 0.5 mg m^{-3}. Levels dropped again to between 0.2 and 0.3 mg m^{-3} in SA/SAF/polar waters. The marked diel variation in the chlorophyll-*a* trace was due to an approximately two-fold change in fluorescence yield. This diel change in fluorescence response is well known, and the magnitude of the diel change is similar to that seen by others [*Marra*, 1997]. No phytoplankton blooms (defined as chlorophyll-a concentrations >1 mg m^{-3}) were seen on the *Southern Surveyor* cruise track except in shelf waters near Hobart.

In contrast, five bloom regions were encountered along *Discoverer's* cruise track. The bloom region west of Cape Grim on DOY 330-333 had the largest areal extent (roughly between 41.4°S- 42°S, 140°E-144°E) and chlorophyll-*a* levels were between 1.0 and 1.5 mg m^{-3}. This was double or triple

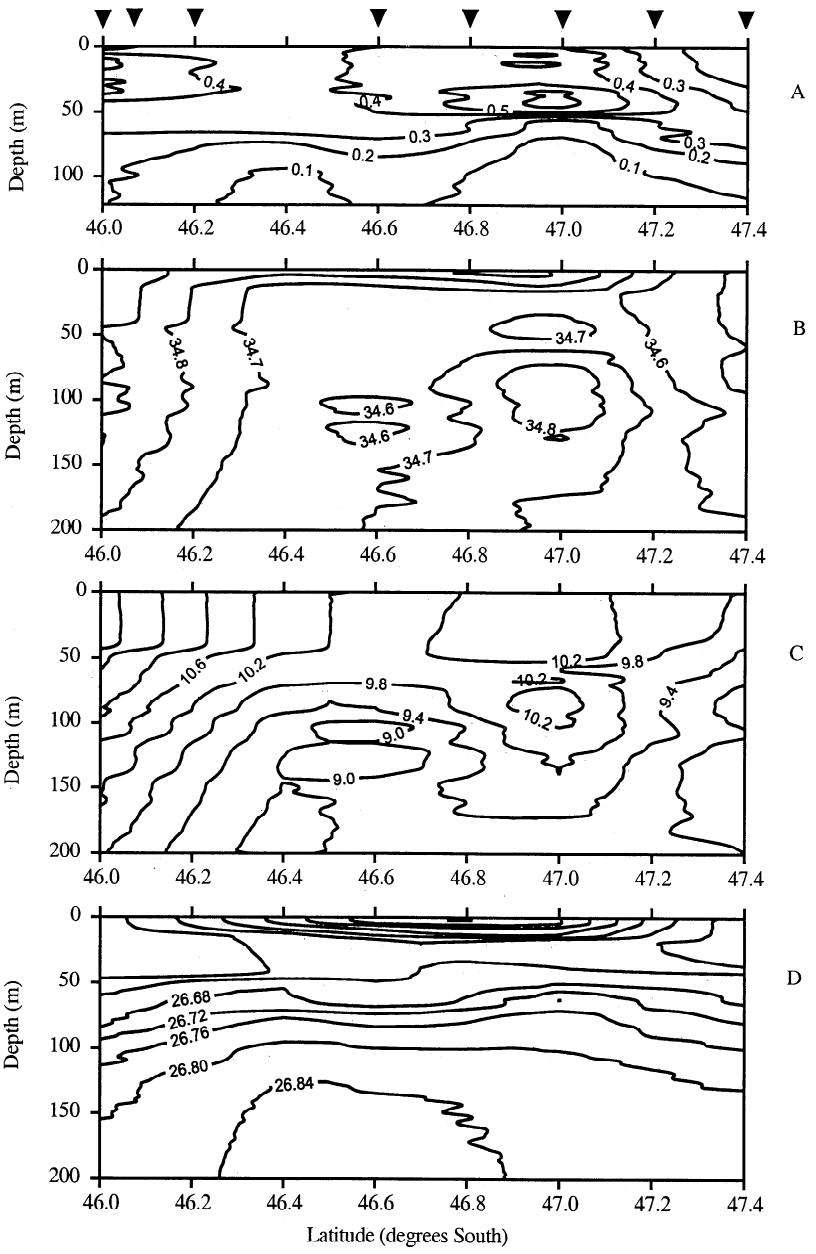

Figure 6. Contours of (a) chlorophyll-a (to 125 m), (b) salinity, (c) temperature, and (d) density (b-d to 200 m) along 150°E between 46.0°S and 47.4°S on DOY 337-339 measured from *Southern Surveyor*. The positions of the CTD stations are indicated by a solid triangle. Contour intervals are chlorophyll-*a*, 0.1 mg m^{-3}; salinity, 0.05 practical salinity units; temperature, 0.4°C; and density, 0.4 sigma-theta units.

the levels found when *Southern Surveyor* was in the area 10 days earlier (Figure 4d). There was a drawdown of >2 μ*M* nitrate in the same period. Four other blooms, apparently much more localized, were crossed on DOY 325, 337, and 345 (in SA waters) and on DOY 343 in polar waters at the end of the Lagrangian B transect.

3.3.2. DMS and ammonia in surface waters, atmosphere and flux rates. *Jones et al.* [1998] reported DMS_{sw} data from Southern Surveyor, and Bates et al. [1998b] have presented mean concentrations of DMS_{sw}, DMS_{atm}, and calculated flux rates in polar, SA, and STCZ waters. There are some interesting patterns in the detail of the measurements made from Discoverer, however. The mean concentrations of DMS_{sw} in Subantarctic waters (Figure 4 g) increased significantly (ANOVA, P >0.001, n = 484) during this experiment. Between DOY 323 and 330, DMS_{sw} concentrations were 0.99 nM (SE 0.048, n = 187), increasing to 1.3 nM (SE 0.057, n = 131) between DOY 333 and 338, and increasing again to 2.3 nM (SE 0.50, n = 169) between DOY 340 and 346. In the STCZ, peaks of DMS_{sw} (>3nM) were seen near Cape Grim on DOY 329-333 and west of Cape Grim on DOY 338-340. The DMS flux (Figure 4h) was highest on DOY 343, when wind speeds averaged 16.8 m s^{-1}. DMS flux and DMS_{atm} increased in the DOY 329-333 interval, probably as a result of moderate winds (mean 10.6 m s^{-1}) and increased DMS_{sw} (Figure 4g). A second period of high DMS_s also in the STCZ, on DOY 338-340, associated with much lower average wind speeds (mean 6.2 m s^{-1}) yielded low flux rates and only a small increase in

DMS_{atm}. Ammonium concentrations in surface seawater $[NHx]_{sw}$ along the Discoverer's cruise track were generally <1 μM (Figure 4l), and there was no systematic variation in concentration with latitude. On DOY 331-334, extraordinarily high peak concentrations of $[NHx]_{sw}$ (>5 μM), flux (12 μM m^{-2} d^{-1}) and $[NH_3]_{atm}$ were measured in and over STCZ water west and south of Cape Grim. Increased concentrations of DMS_{sw}, DMS_{atm}, chlorophyll-a, and an increased DMS flux were present in this period. The high flux rates (Figure 4k) seen on DOY 343-347 were not reflected in elevated atmospheric NH_3 (Figure 4l). The interaction between seawater concentrations, flux rates, wind speed, and atmospheric concentrations of both DMS and NH_3 is clearly not simple.

3.4. Surface Water Masses, Chlorophyll-*a*, Ammonia, and DMS Along the Tracks of the Lagrangian "A" and "B" experiments

3.4.1. Lagrangian A Experiment (DOY 335-337). During the Lagrangian A experiment, the two research vessels sampled along a track between 45°S, 141°E and 47°S, 152.35°E between DOY 335 and 337 (Plate 1), following actual and calculated balloon trajectories. The *Discoverer* transect started on DOY 335 in SA water at 45°S, 141°E and crossed into STCZ water near 46°S, 148°E, finishing on DOY 336. Aircraft flight 18 followed the *Discoverer*'s track closely. The *Southern Surveyor* transect started in STCZ water on DOY 336 at 46.5°S, 148°E, crossed into SA water at about 150.3°E, and ended at 47.0°S, 152.35°E on DOY 337. Aircraft flight 19 covered the *Southern Surveyor* transect, whilst flight 20 took place over Subantarctic water and the Subantarctic Front region between 52°S–54°S, 156°E–158°E. Chlorophyll-*a* values along the western end of the transect (0.5–0.7 mg m^{-3}) increased with salinity to peak at 1.1 mg m^{-3} near 148°E (Figure 4d). Along the *Southern Surveyor* transect surface chlorophyll-*a* values (Figure 3c) ranged between 0.6and 0.8 mg m^{-3} in STCZ water at the western end to between 0.2 and 0.5 mg m^{-3} in the SA water at the eastern end. Seawater and atmospheric DMS concentrations were relatively low and constant along the *Discoverer* transect (Figures 4g and 4i). *Jones et al.* [1998] found increases in seawater dimethlysulphoniopropionate (70–100 n*M*) and dimethyl sulphide (0.7–4.0 n*M*) concentrations as *Southern Surveyor* traveled eastward, and these concentrations were inversely correlated with chlorophyll-*a*.

3.4.2. Lagrangian B experiment (DOY 342-343). On DOY 342, *Discoverer* started sampling in SA water at 45.5°S, 144.0°E and finished in the SAF (47°S, 146.1°E) on the first day of the Lagrangian B experiment and then moved southeast to 49.1°S, 147.7°E in the SAF/PF zone on DOY 343. The first two aircraft flights (flights 24 and 25) covered the area between 45°S–47°S, 143°E–146.5°E [*Bates et al.*, 1998], over STCZ water although quite close to the front between the STCZ and SA water masses. Flight 26 covered the area between 49.5°S–52°S and 147.5°S–148.5°E over the SAF/PF meander zone, close to the ship's track on DOY 343.

Chlorophyll-*a* concentrations in the surface waters doubled between 45.5°S, 144°E and 47°S, 146°E, and increased dramatically to peak at 2.1 mg m^{-3} at 49.1°S, 147.7°E (Figure 4c). Seawater DMS decreased along transect 1, but increased to ~6 n*M* in the SAF/PF zone on DOY 343 (Figure 4g). Atmospheric DMS and the flux of DMS to the atmosphere also followed this same pattern (Figures 4h and 4i). Nitrate concentrations (Figure 4e) dropped, whilst ammonia concentrations (Figure 4j) increased in surface waters on the first transect during DOY 342. This pattern reversed during DOY 343, as the vessel entered the SAF/PF zone. The ammonia flux was about 7 n*M* m^{-2} d^{-1} (Figure 4l) in this region, although atmospheric ammonia concentrations were quite low (<2 n*M* m^{-3}).

Ship-based measurements show the areas covered during both Lagrangian experiments were over oceanographically complex areas. The atmospheric concentrations of DMS, ammonia, and other compounds will represent an integrated signal from the various water masses.

3.5. Nutrients, Chlorophyll-*a*, Primary Production, Phytoplankton Growth Rates and Microzooplankton Grazing Rates in the Western Region during the ACE 1 Intensive

3.5.1. Nutrients. Nitrate and silicate concentrations to a depth of 200 m along the north-south transect are shown in Figure 7. Low levels of silicate (<1 μ*M*) were found in STCZ surface waters, and there was a gradual increase in silicate with depth and latitude until the northern edge of the polar front was reached near 52°S (Figure 7a). Silicate levels increased sharply to >10 μ*M* in surface waters in the polar frontal region, and >30 μ*M* at 200 m. A parcel of relatively high silicate water (~8 μ*M*) was seen at about 100 m on the northern edge of the cold-core eddy. The nitrate distribution followed the silicate pattern, with lowest nitrate levels (<6 μ*M*) at 42°S in the surface water of the STCZ region (Figure 7b). Nitrate in the SA increased with increasing latitude reflecting the deep winter mixing. Nitrate concentrations rose from about 20 μ*M* just north of the SAF front to >24 μ*M* in the polar water mass. There was high nitrate water at depths of 100-200 m intruding north to ~46°S with a parcel of >20 μ*M* water on the northern edge of the cold-core eddy (Figure 7b). At the northern end of this transect, phosphate concentrations (not shown) were >0.3 μ*M* in the surface STCZ water and increased to >1 μ*M* below 50 m. South of the SAF, phosphate levels were >1.4 μ*M* in surface waters. The concentrations of these three nutrients are in agreement with the expected pattern for this region and season [*Sedwick et al.*, 1997; *Clementson et al.*, 1998; *Maeda et al.*, 1985; *Yamamoto*, 1986].

Surface and mixed layer ammonia concentrations were generally <100 n*M* south of 48°S, but >100 n*M* north of 48°S. Ammonia concentrations in the upper 200 m along this transect were highest at depths between 50 and 80 m in STCZ and SA water (Figure 7c), but at depths >120 m in polar waters. At the Cape Grim site (40.8°S, 143.4°E), ammonia levels in the mixed layer (not shown) were <160 n*M* but peaked at 455 n*M* at 80 m. High ammonia levels were associated with the base of the mixed layer only at 42°S: at the other stations peak ammonia concentrations were much deeper. The increased ammonia concentrations measured from *Southern Surveyor* at 42°S and 45°S correspond to the region of high seawater and atmospheric ammonia levels, and large sea-air flux of ammonia measured on R/V *Discoverer* in the same general area about 9 days later (DOY 332, Figures 4j, 4k and 4l).

3.5.2. Chlorophyll-*a*. The chlorophyll-*a* distribution along the north-south transect is given in Figure 7d. In the STCZ, chlorophyll-*a* maxima were generally above 50 m in the mixed layer. In the SAZ, highest values were found below

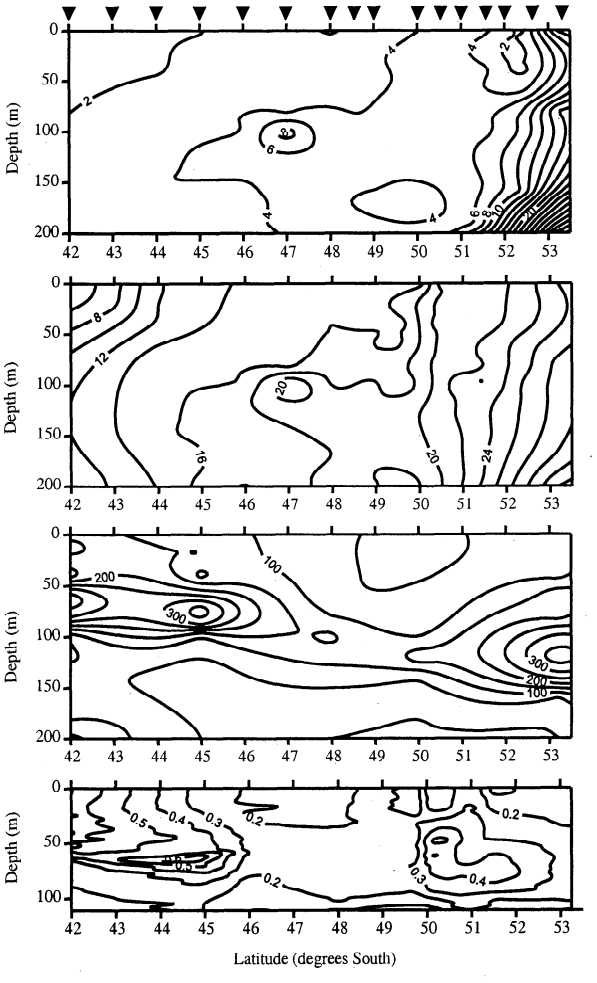

Figure 7. Contours of (a) silicate, (b) nitrate, and (c) ammonia between the surface and 200 m and for (d) chlorophyll-*a* between the surface and 125 m along the western transect occupied by *Southern Surveyor* (42°S, 140°E and 53.5°S, 145.5°E). The position of the CTD stations are indicated by a solid triangle. The contour intervals are silicate and nitrate, 2 μM; ammonia, 50 nM, and for chlorophyll-*a*, 0.1 mg m^{-3}. The patch of high nitrate, high silicate water present at about 100 m depth near 48°S is on the northern edge of the cold-core eddy.

the mixed layer (50–80 m) near the 1% light depth. The depth of the chlorophyll-*a* maxima also tended to be shallower than the depth of the highest ammonia levels. Peak values were <0.8 mg m^{-3} and are somewhat higher than values near 0.5 mg m^{-3} reported by *Sedwick et al.* [1997] for the same region in January 1995. Total column chlorophyll-*a* (between the surface and 110 m) dropped sharply between 45°S and 46°S, and increased in the SAF region at about 50°S (Table 2). Column chlorophyll-*a* dropped again at 51.4°S, and then increased, especially below 60 m, at 53.3°S.

3.5.3. Primary production. Primary production was measured off the shelf near Cape Grim, and along the north-south transect from 42°S, 140°E to 53.3°S, 145.5°E between DOY 323 and 334. The 1% light depth was greater than the mixed layer depth at all sites except 50°S, 145.5°E. The highest modeled daily primary productivity (3200 mg carbon m^{-2} d^{-1}, Table 2) was found just off the shelf break near Cape Grim at 40.8°S, 143.7°E. Most of the modeled production at this site occurred in the mixed layer, and the mixed layer photosynthetic capacity was very high (~97 mg carbon (mg Chl a)$^{-1}$ d^{-1}). Along the latitudinal transect, the highest modeled productivity was at 42°S, 140°E in the northern edge of the Subtropical Convergence Zone, again most of the production at this site occurred in the mixed layer. In the Subantarctic zone, most of the modeled primary production was occurring below the very shallow mixed layer (<10 m). The moderate levels of modeled production found at 45°S and 46°S suggest the spring bloom was just starting at these latitudes (Table 2). At 48°S, modeled production in the cold-core eddy was considerably lower than just outside the eddy. In the PF/polar waters, modeled production estimates were between 410 and 830 mg C m^{-2} d^{-1}. At the 53°S site, modeled production increases about 50% (from 540 to 830 mg C m^{-2} d^{-1}) on successive days.

In surface waters, photosynthetic efficiencies in ST waters were very high (11.0-11.4 mg C (mg Chl a)$^{-1}$ h^{-1}. Photosynthetic efficiencies in surface waters along the rest of the transect ranged between 2.5 and 6.8 mg C (mg Chl a)$^{-1}$ h^{-1}, with no significant difference between water masses.

3.5.4. Phytoplankton growth and microzooplankton grazing rates. Phytoplankton growth rates, calculated from the net ^{14}C production results in and below the mixed layer, are given in Table 2. Mixed layer growth rates were moderate, between 0.42 d^{-1} and 0.83 d^{-1}, along the western transect between 42°S and 48°S, and decreasing below 0.35 d^{-1} in the SAF/PF region, but increasing in one of the two estimates at 53.3°S, 145.5°E. In the eastern block, mixed layer growth rates were a little higher (0.75 d^{-1} to 1.1 d^{-1}). Growth rates below the mixed layer were quite low, reaching a maximum of only 0.35 d^{-1} at 46°S, 143.6°E, and tended to be negative when the mixed layer was deeper than about 40 m, or about the 10% light depth. These negative growth rates are due to the respiration of the substantial phytoplankton biomass exceeding the light-limited rate of primary production.

Phytoplankton growth rates at 42°S, 140°E could also be calculated using changes in chlorophyll-a concentration at 5 m depth between DOY 323 and 324 (*Southern Surveyor* underway data) and between these days and DOY 330 (*Discoverer* underway data). The chlorophyll profiles on DOY 324 and 330 (Figure 8) show the increase in chlorophyll-*a* was uniform in the mixed layer. Between DOY 323 and 324, the chlorophyll-*a* concentration had increased from 0.62 to 0.68 mg m^{-3}, but on DOY 330, had increased again to 1.1 mg m^{-3}. Using the Parsons and Takahashi equation referred to earlier, the growth rate between DOY 323 and 324 was 0.09 d^{-1}, and over the 6 and 7 day interval to DOY 330, the rates were 0.075 and 0.08 d^{-1} respectively. These values are similar to the net growth rate of 0.07 d^{-1} (Table 2) calculated from the grazing dilution experiment at this site on DOY 323. These rates are considerably lower than the rates calculated from the mixed layer, modeled primary production at this site (Table 2).

Jones et al. [1998] have reported the microzooplankton grazing rates from the grazing dilution experiments carried out on *Southern Surveyor* during the ACE 1 experiment. The phytoplankton growth rates measured in these experiments and the net rate of population change (growth rate minus grazing rate) are shown in Table 2. The specific growth rates obtained from the grazing dilution experiments were higher than rates estimated from the ^{14}C experiments in SA waters,

but less than the rates in PF and polar waters. At 46.6°S, 149.23°E, the growth rate from the grazing dilution experiment was only half the rate estimated from the ^{14}C method. The net rate of population change showed low to moderate increases in phytoplankton populations between 40.8°S and 50°S in the western block, and grazer control reducing the phytoplankton population at 53.30°S, 145.5°E and at 46.6°S, 149.2°E.

3.6. Nutrients, Chlorophylls, Primary Production, Phytoplankton Growth Rates, and Microzooplankton Grazing Rates in the Eastern Region During the ACE 1 Intensive

3.6.1. Nutrients, DMS, and chlorophyll-a in the eastern region on DOY 319-325. The water masses crossed in this period are discussed above (section 3.2.3). In STCZ water, surface nitrate increased from <8 μ*M* to >9 μM and increased again in SA water to >10 μ*M*. In polar waters, nitrate increased to about 16 μM, but increased to be >20 μ*M* near Macquarie Island. Surface chlorophyll-a (Figure 4d) did not change greatly in different water masses until a bloom (>1 mg m^{-3}) was crossed on DOY 325 in SA water. DMS_{sw}, DMS flux, and DMS_{atm} were all very low during this period (Figures 4g, 4h, and 4I). No ammonia data were available until DOY 325.

3.6.2. Nutrients and ammonia in the eastern region on DOY 338-340. Surface nitrate values were >10 μ*M* for at all stations except 46°S, where the value was only 6 μ*M* (Figure 9a). Phosphate concentrations (not shown) were about 0.6 μ*M* in surface waters at 46°S, and increased to >1.0 μ*M* at 47.4°S. Mixed layer silicate concentrations were < 1μ*M* in STCZ water, increasing to 2 μ*M* in SAZ surface water at 47.3°S (Figure 9b). Silicate concentrations increased to about 4 μ*M* below the mixed layer, reflecting the northward intrusion of the SA water. Ammonia distributions were highest in STCZ water at the northernmost station (Figure 9c), reaching a peak of 750 n*M* at 60 m depth. Ammonia levels decreased both in and below the mixed layer as latitude increased, and levels were below detection limits (20 n*M*) at 100 m at both 47°S and 47.4°S. At 46.6°S, 149.2°E, on DOY 339, silicate levels were similar to those seen at 46.6°S, 150°E, but nitrate concentrations were lower, and ammonia concentrations below the mixed layer were considerably higher (Figure 9).

3.6.3. Chlorophyll-a, primary production and microzooplankton growth and grazing along 149°E and 150°E. There was a substantial subsurface chlorophyll-a maximum (>0.50 mg m^{-3}) between 35 m and 50 m depth in water with a salinity >34.7. This maximum is below the surface mixed layer, but above the lens of STCZ water found between 70 m and 150 m. In the chlorophyll-a maximum, ammonia and silicate levels were comparatively low, and there was an apparent drawdown of about 1 μM nitrate compared to nitrate concentrations above and below the chlorophyll-a maximum.

The rate of modeled primary production was quite high (>975 mg C m^{-2} d^{-1}) along the 150°E transect. On the basis of the salinity underneath the warm, salty cap, the site at 46°S, 150°E was in the STCZ, while the other two sites where primary production was measured were in SA water. Mixed layer depths at the three sites ranged between 35 m and 45 m, with more than 50% of the modeled primary production occurring in the mixed layer. No grazing experiments were made on this transect. Nearby, at 46.6°S, 149.23°E, the mean

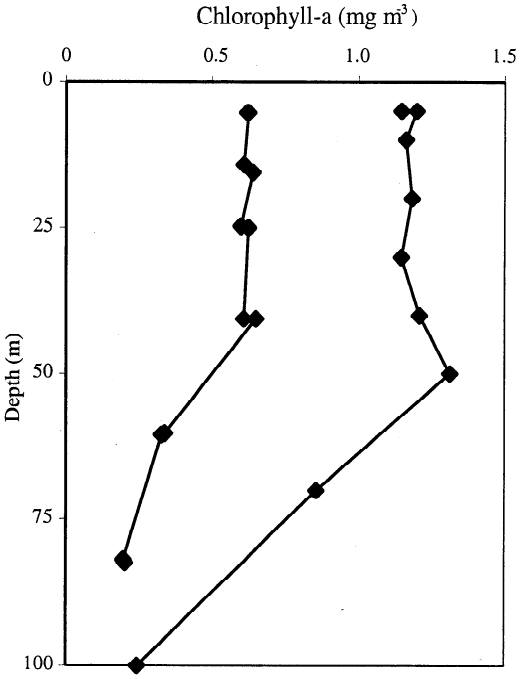

Figure 8. Chlorophyll-*a* (mg m^{-3}) profiles made on DOY 323 by *Discoverer* (solid diamonds) and *Southern Surveyor* (solid squares) on DOY 330 at 42°S, 140°E. The surface values were used for the growth rate comparisons.

modeled column production (two replicates done 5 hours apart; Table 2) was 1953 mg C m^{-2} d^{-1}, with most of the production occurring in shallow mixed layers. These rates were similar to the very high rates found in the STCZ at 42°S, 140°E earlier in the cruise. The microzooplankton grazing rate was greater than the phytoplankton growth rate (Table 2) at this site.

4. Discussion

4.1. Water Mass Distribution

Water mass boundaries in this region have previously been identified based on the subsurface physical oceanographic structure but this is not useful for work concentrating on mixed layer processes [e.g., *Rintoul et al.*, 1997]. In this paper, the mixed-layer, salinity front definitions approximately correspond to these subsurface temperature/depth combinations and are most useful for defining the water mass boundaries. The salinity boundaries were not coincident with the major surface temperature fronts. *Harris et al.* [1991] also made this same observation. The one feature that is constant, at least between 140°E and 145°E, is the position of the SAF/PF [*Rintoul et al.*, 1997; *Sedwick et al.*, 1997; *Clementson et al.*, 1998]. The boundary between the STCZ and SAF water west of Tasmania can shift depending on year and season (*Clementson et al.*, 1998]. The structure to the east of Tasmania is much more complex than to the east of 147.5°E (Figure 6). For example, *Clementson et al.* [1998] describe a warm salty cap intruding southward overlying the cooler, less salty Subantarctic water formed by winter cooling. This shallow mixed layer, combined with elevated nitrate concentrations, led to an increase in phytoplankton standing stocks and primary production rates. This is similar to the structure

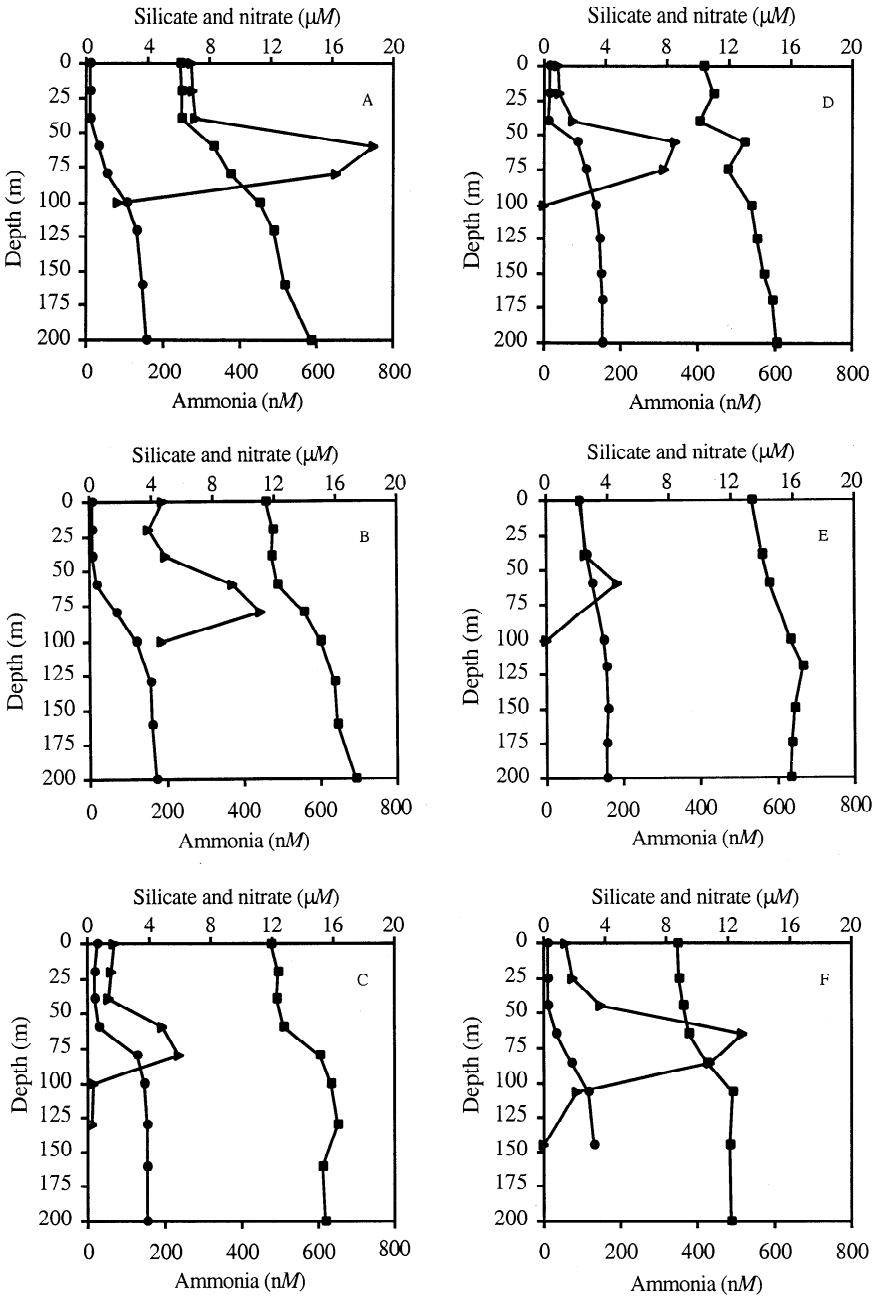

Figure 9. Profiles of nitrate (solid squares), silicate (solid circles) and ammonia (solid triangles) in the upper 200 m along the eastern transect between 46.0°S and 47.4°S, along 150°E on DOY 337-339, and at 46.6°S, 149.2°E taken from *Southern Surveyor*. Nitrate and silicate concentrations (μM) are plotted against the top scale, and ammonia concentration (nM) is plotted against the bottom scale. Latitudes (a) 46°S, (b) 46.3°S, (c) 46.6°S, (d) 47.0°S, and (e) 47.3°S are shown along 150°E. Profile (f) was at 46.6°S, 149.2°E.

observed during ACE 1 in the eastern block region. In contrast, *Furuya et al.* [1986] saw a different structure, with cool, less saline Subantarctic water overlying subducted subtropical convergence zone water. They too saw increased chlorophyll and primary production rates but in this instance, it was in the Subantarctic water cap. These different structures point to the intense mesoscale variability in the region east of Tasmania, and *Morrow et al.* [1992] show these are driven by the influence of the East Australian Current, the zonal Antarctic Circumpolar Current and the topography.

4.2. Nutrients

The north-south gradient in silicate in the different water masses observed during ACE 1 is commonly seen in this region [*Furuya et al.*, 1986; *Maeda et al.*, 1985; *Clementson et al.*, 1998]. East-west differences in structure within a water mass (Figures 3d, 3e, and Figure 4e) may reflect spatial variation in biological demand if the spring bloom was further advanced in one locality compared with another locality.

Nitrate concentrations in the mixed layer exceeded silicate concentrations in the study region except on the northern side of the cold-core eddy at 48.5°S, 145.5°E. This low silicate to nitrate ratio is a common feature in this region [*Maeda et al.,* 1985; *Yamamoto,* 1986; *Sedwick et al.,* 1997], especially in SA and Polar waters. The low silicate: nitrate ratios (~ 0.2-0.4) suggest silicate was limiting diatom growth in the mixed layer in line with *Richards* [1958]. However, more recent work has shown strong deviations from this ratio [e.g., *Minas and Minas*, 1992] do occur. *Hutchins and Bruland* [1998] argue that diatoms stressed by a lack of iron should deplete surface waters of silicate before nitrate, leading to a secondary silicate limitation of phytoplankton communities. *Sedwick et al.* [1997] found dissolved iron levels were <0.8 n*M* in STCZ, SA, and polar waters along 140°E. *Kamykowski* and *Zentara* [1989] have suggested that iron deficiency could limit nitrate utilization in the Southern Ocean when ammonia levels are below 2 μ*M*. During the ACE 1 intensive, ammonia concentrations only exceeded 2 μ*M* in surface waters near 41°S on DOY 331-334, and did not exceed 1 μ*M* in the mixed layer at any other time. If we assume similar iron levels, and given the low ammonia levels measured, then silicate would have been preferentially taken up by diatoms, leading to the observed silicate depletion and nitrate excess in SA and polar waters.

Phytoplankton community structure in Subantarctic and polar waters changes from diatom-dominated communities in December to dinoflagellate- and coccolithophorid-dominated communities with some diatoms present in January/February [*Yamamoto,* 1986; *Holm-Hansen et al.*, 1977; *Hara and Tanoue,* 1985]. *Jones et al.* [1998] found diatoms dominated phytoplankton biomass at 40°S and 41°S, and at 52°S and 53°S. Dinoflagellates belonging to the genera *Gymnodinium, Protoperidinium*, and *Exuviaella* dominated phytoplankton biomass at the other sites on the north-south transect. On the north-south transect, they found chlorophyll-*a* was negatively correlated with dinoflagellate biomass, but positively correlated with diatom biomass. This suggests holozoic and heterotrophic dinoflagellates were making up most of the dinoflagellate biomass. In open ocean waters, *Protoperidinium* spp. and *Gymnodinium* spp. are known to be holozoic [*Steidinger and Tangen* 1997]. We believe that the dominance of the holozoic and heterotrophic dinoflagellates reflect the "winter" community and the spring bloom had not yet started between 42°S and 50°S during the ACE 1 experiment.

4.3. Distribution of Chlorophyll-a in Water Masses

Surface chlorophyll-*a* values were broadly comparable to those found by other authors [*Clementson et al.*, 1998; *Furuya et al.*, 1986; *Yamamoto,* 1986] for equivalent water masses and months, except they did not encounter any blooms (> 1 mg chlorophyll-a m^{-3}). Surface chlorophyll-*a* concentrations in ST and SA waters near New Zealand were similar to our results, although the chlorophyll-a concentrations during the spring bloom in STC waters were somewhat greater that we found [*Bradford-Grieve et al.,* 1997]. Column chlorophylls in both the eastern and western sectors are higher (Table 2) than the 25-31 mg m^{-2} reported by *Clementson et al.* [1998] in STCZ water between 43°S and 49°S along 152°E during January 1990. Peak chlorophyll-a values found by *Clementson et al.* [1998] were only about 0.5 mg m^{-3}, again quite low compared to our results. This difference is most likely due to seasonal effects, with the spring bloom beginning during the latter part of the ACE 1 experiment, but nearly completed when *Clementson et al.* [1998] were sampling. In the Subtropical zone west of New Zealand, *Bradford and Chang* [1987] found integrated column chlorophyll values (0-100 m) in the range of 20–58 mg m^{-2}, with peak chlorophyll-*a* values up to 3.4 mg m^{-3}. In October, over the Chatham Rise region east of New Zealand, *Bradford-Grieve et al.* [1997] reported column chlorophylls averaged 46 mg m^{-2} in ST waters. This average was very close to the 49 mg m^{-2} we found during the ACE 1 experiment. In the STCZ, the column-integrated mean value of 110 mg m^{-2} reported by *Bradford-Grieve et al.* [1997] is about 3 times greater than the mean of 32 mg m^{-2} found during ACE 1 and considerably higher than levels found by *Clementson et al.*, [1998]. In the SAZ, we found column chlorophyll-a values of 43 mg m^{-2}, some three times higher than the 14 mg m^{-2} reported by *Bradford-Grieve et al.* [1997]. These differences and similarities all highlight the difficulties in generalizing water column properties in this region.

4.4. Primary Production

The modeled primary production results reported here and by *Parslow et al.* [1996] are somewhat higher than those reported by most other authors working in this region. *Parslow et al.* [1996], using the same P-I method and column production model as we used here, calculated a daily column production at 44.6°S, 145.9°E in the STCZ of 2600 mg C m^{-2} d^{-1} in November, and about 1300 mg C m^{-2} d^{-1} in February. They measured photosynthetic efficiencies in surface waters of 4.2 and 3.8 mg C (mg Chl *a*)$^{-1}$ h^{-1}, respectively. *Holm-Hansen et al.* [1977] found carbon fixation rates were 260, 60-105, and only 26 mg m^{-2} d^{-1} in the Subtropical Convergence Zone, the Subantarctic Front, and polar zone, respectively, in March along 150°E. *Clementson et al.* [1998] found column production along 152°E in January ranged between about 260 and 460 mg C m^{-2} d^{-1}, with no strong latitudinal gradient in the STCZ waters sampled. *Harris et al.* [1987] reported potential productivity of 1.0-2.2 mg C m^{-3} h^{-1} and column carbon fixation rates in the range of 270-580 mg C m^{-2} d^{-1} on the shelf and shelf break near Cape Grim in late October. *Jitts* [CSIRO, 1963] calculated column carbon fixation rates in the range of 260-460 mg C m^{-2} d^{-1} between 44.5°S and 45°S in STCZ waters, with no consistent latitudinal pattern in depth-integrated production.

In October, east of New Zealand, column carbon fixation rates in ST waters averaged 970 mg C m^{-2} d^{-1}, and 990 mg C m^{-2} d^{-1} in the STCZ, while production in SA waters averaged 250 mg C m^{-2} d^{-1} [*Bradford-Grieve et al.,* 1997]. *Vincent et al.* [1989] suggested that water column production was controlled by the interplay between variations in the light limitation parameter alpha, from the P-I curve, and the mean annual irradiance. It may be that the difference between our results, and those of *Bradford-Grieve et al.* [1997] were due in part to differences in daily irradiance. *Downer and Lucas* [1993] estimated column carbon fixation rates in ST water inside a warm-core eddy south of South Africa at 240-310 mg C m^{-2} d^{-1} but found higher levels (250-440 mg C m^{-2} d^{-1}) in Subantarctic waters surrounding the eddy. These photosynthetic capacities and column production rates are somewhat lower although chlorophyll biomass was higher than we measured. *Hosaka and Nemoto* [1986], *Yamamoto* [1986], and *Furuya et al.* [1986] found surface carbon fixation rates in the STCZ

along 150°E varied between 0.25 and 1.7 mg C m^{-3} h^{-1}, and assimilation numbers ranged between 1.1 and 13 mg C (mg Chl *a*) $^{-1}$ h^{-1}. In the SA/SAF region, these same authors found carbon fixation rates were between 0.3 and 1.5 mg C m^{-3} h^{-1}, and assimilation numbers varied between 3.2 and 8.4 mg C (mg Chl *a*) $^{-1}$ h^{-1}. South of South Africa, *Laubscher et al.* [1993] found phytoplankton blooms (>2 mg Chl *a* m^{-3}) in surface waters at the Subtropical, Subantarctic, and polar fronts, with photosynthetic capacities of 1.3, 0.75, and 1.15 mg C (mg Chl *a*) $^{-1}$ h^{-1}, respectively, in each region. These rates are similar to those obtained by *Allanson et al.* [1981] in water masses between these fronts.

Comparison of photosynthetic parameters and rates from other regions determined by different methods of estimating these parameters and rates can be difficult. *Dring and Jewson* [1982] note that short incubations (duration ~1 hour) provide estimates that may be closer to gross carbon uptake rate than long incubations because the fraction of labeled carbon being respired to CO_2 and/or recycled within the cell increases with the duration of the incubation. *Sakshaug et al.* [1997] suggest that estimates of photosynthetic parameters from a photosynthetron using small, whole-water samples [e.g., *Lewis and Smith,* 1983] or by our method should lead to higher estimates of productivity than those from other incubators which involve longer incubation times, filtering of samples, and no determination of DOC. *Riemann and Jensen* [1991] found primary production measured using an acidification and bubbling technique gave estimates of production that were about 1.4 times higher than production estimates obtained by a particulate filtration procedure. They argue that the difference is due to dissolved organic carbon produced by the phytoplankton, and thus the acidification and bubbling method results in an approximation of total primary production.

Sullivan et al. [1993] used CZCS imagery to show comparatively low standing stocks of phytoplankton in the region between 30°S and 50°S in the western Indian Ocean and note this is coincident with a zonal region of high wind stress and deep mixed layers. *Mitchell et al.* [1991] argue that low standing stocks in the Antarctic Circumpolar Current are due to low growth rates caused by low average irradiances in deep mixed layers and loss terms, such as sinking and grazing, that can exceed the rate of growth. Our results show that the deep chlorophyll maxima in SA and polar waters [Figures 6d, 7a, and 9] are not detected by the ocean color satellites and the satellite images are underestimating the true standing stock of phytoplankton, and probably the potential production.

4.5. Phytoplankton Growth and Microzooplankton GrazingRates

Growth rates estimated from the modeled daily primary production assume that the C:chlorophyll-*a* ratios and respiration rates are not impacted by different temperatures, nutrient concentrations, mixed layer depths, light climate, and community structure [e.g., *Bradford-Grieve et al.,* 1997]. In a region as oceanographically complex as the ACE 1 region, these assumptions must be treated with some caution. However, the growth rates we calculated from the modeled daily primary production are higher than the average 0.27 d^{-1} found by *Clementson et al.* [1998] along 152°E. They are at the lower end of the range of the 0.73-1.8 d^{-1} found by *Bradford-Grieve et al.* [1997] in ST, subtropical front, and SA waters east of New Zealand in October in or at the end of the spring bloom. As nitrate in most of the ACE 1 region (except the ST water on DOY 331-334) was still relatively high, with increasing chlorophyll-a levels; it appears the spring bloom was just beginning in December 1995.

A comparison between the growth rates from the grazing dilution experiments and the modeled daily production data is difficult. This is because the former is based on the net change in chlorophyll-a concentration after being enriched with ammonia, and the latter is based on calculated net fixed carbon. The modeled net primary production calculation assumed a 10% respiration figure and an indicative chlorophyll to carbon ratio of 50 [*Geider,* 1987]. The mixed layer growth rates estimated from the modeled primary production at the same site on successive days could be either quite similar (48°S, 50°S), or up to a factor of 2 different (46.6°S, 149.2°E, Table 2). Changes in mixed layer depth or mixed layer chlorophyll did not seem to contribute to this variation. In the PF/polar water samples, the increased growth rates, seen when ammonia was added in the grazing dilution incubations, suggest that ammonia may have been one factor limiting growth in these regions. For example, ammonia concentrations at 25 m were <250 n*M* (Figure 7c). Overall, the picture is one of moderate increases in the phytoplankton populations in the STCZ and SA water along the main western transect, while grazers were controlling phytoplankton biomass at 53°S and in the eastern block.

Grazing rates and growth rates at 40.8°S, 149.2°E on DOY 323-324 were tightly coupled, with a net rate of phytoplankton population increase of only 0.07 d^{-1}. On DOY 332-334 at this site, there were high levels of DMS in seawater, elevated atmospheric DMS concentrations, and an increase in the calculated DMS flux (Figure 4). Seawater and atmospheric ammonium concentrations and calculated ammonium flux were the highest measured during the ACE 1 intensive experiment. At 46°S, 149.2°E, grazing rates exceeded growth rates (Table 2), and increases in seawater and atmospheric DMS and DMS flux were observed. There was only a slight increase in atmospheric ammonium and calculated ammonium flux. In polar waters, however, where the highest microzooplankton grazing rates were measured, there was no similar increase in DMS or ammonia in seawater or in the atmosphere. *Jones et al.* [1998], working on *Southern Surveyor*, concluded that there was a link between microzooplankton grazing and DMS in the diatom dominated Polar waters, but not the dinoflagellate-dominated STCZ waters. The apparent correlation between high microzooplankton grazing rates in ST and STCZ waters, and the high seawater concentrations of DMS observed suggest that the link does exist.

Sunda and Huntsman [1997] argue that interactions among iron availability, light limitation, and cell size determine marine phytoplankton growth rates. They state that the combination of low iron and light limitation, commonly seen in deep chlorophyll-*a* maxima, will favor the growth of small cells, and hence lead to an increase in microzooplankton grazing rates. *Sedwick et al.* [1997] have shown that dissolved iron concentrations in the mixed layer ranged from 0.5 n*M* at 40°S to a fairly uniform 0.21-0.25 n*M* between 45°S and 50°S, and were 0.26 n*M* at 53°S along 140°E in January 1995. There was no evidence for enrichment from deeper in the water column. Total dissolvable iron was 0.59 n*M* at 45°S, decreasing to 0.19 n*M* at 50°S, and increased to 0.37 n*M* at 53°S. The cruise tracks of *Southern Surveyor* cruise SS 1/95, and SS 11/95 were very similar, and as the only source of iron

could be atmospheric deposition, we suggest that iron levels were probably similar on the two cruises.

Growth and grazing rates measured by the grazing dilution method did not show any consistent pattern with latitude. The highest growth and grazing rates were measured at 53.3°S where *Sedwick et al.* [1997] found iron concentrations of 0.25 n*M*. In the mixed layer, growth rates estimated from the column production data do show a decrease with latitude and hence with PAR, even though iron levels did not change greatly in January 1997 south of 45°S [*Sedwick et al.,* 1997]. The picture is complicated by the decrease in potential maximum growth rates with temperature [*Eppley,* 1972]: how this enters the iron/light equation has not been examined. Growth rates estimated from the column production data (Table 2) show that growth below the mixed layer is often negative, or close to zero. This could be a field example of growth and production being limited by the interaction of low iron and light, as predicted by *Sunda and Huntsman* [1997]. It does seem as if phytoplankton growth rates could have been iron-limited, but not necessarily light-limited, except below the mixed layer during November-December 1995. This limitation may be affecting nitrogen dynamics in the mixed layer, and fluxes of DMS and ammonia to the atmosphere.

The flux of DMS to the atmosphere is affected by wind speed and the seawater DMS concentration in the mixed layer which, in turn, is affected by phytoplankton production, growth rates, biomass, grazing rates, and microbial consumption rates. Mixed layer depths were mostly shallower than the 1% light depth. The flux of ammonia is affected mainly by $[NH_x]$ concentration, which, in turn, is probably produced by bacteria and is actively taken up by phytoplankton.

There are at least two ways that high DMS concentrations below the mixed layer could accumulate. In SA and polar waters, there is a persistent deep chlorophyll maximum, which sits just below the base of the mixed layer, and deepens as the mixed layer deepens during summer [*Sedwick et al.,* 1997; F. B. Griffiths et al., manuscript in preparation, 1999]. The deep chlorophyll maximum is made up of diatoms and dinoflagellates [S. W. Wright et al., manuscript in preparation, 1999;; R. M. Greene et al., manuscript in preparation, 1999). Grazing and senescence in this layer could lead to DMSP and DMS release and accumulation under the mixed *layer* [*Curran et al.,* 1998; *G. B.* Jones and M. A. J. Curran, manuscript in preparation, 1999]. When wind mixing erodes the base of the mixed layer, DMS and DMSP from below the mixed layer will be mixed upward, into the mixed layer and available to be transferred to the atmosphere. The second mechanism is more relevant to the eastern region, where lenses of STZC or SA water, and the phytoplankton communities contained in them, are being advected on top of each other [*Furuya et al.,* 1986; *Clementson et al.,* 1998]. If a high biomass community in, for example, SA water was advected below STCZ water, we could have a high biomass community cutoff from the surface. When the stratification between these two layers is broken down, any accumulated DMS or DMSP or their degradation products will be mixed into the mixed layer, and again be available for outgassing to the atmosphere. *Jones et al.* [1998] saw large pulses of DMS in the water column, which they linked to microzooplankton grazing. The pulses may also be linked to wind mixing and the mechanisms postulated above, but we do not have the temporal coverage to determine this.

5. Summary

This study has described the physical, chemical, and biological oceanography in the ACE 1 intensive experiment in November-December 1995. The region was oceanographically complex, with intense mesoscale activity that did not provide simple boundaries between water masses. Mixed layer salinities, rather than temperatures, were used to separate the four main water masses because mixed layer salinity is a more conservative property. Temperature displays both a latitudinal gradient and a strong seasonal cycle that is not well characterized. Each of the four water masses sampled (subtropical, Subtropical Convergence Zone, Subantarctic, and polar) have characteristic nutrient concentrations in the mixed layer. Nitrate concentrations increased from about 2 μ*M* to >25 μ*M*, and silicate increased from about 0.5 μ*M* to >12 μ*M* from the subtropical to polar water masses. Nitrate concentrations were high enough not to limit phytoplankton growth, but silicate may have been limiting diatom growth in ST, STCZ, and SA water masses. Vertical profiles showed ammonia concentrations were highest near the thermocline and were generally <200 n*M* in the surface waters. Mixed layer ammonia concentrations decreased as latitude increased up to the polar front. Near Cape Grim, midway through the experiment, very high concentrations (1 μ*M* to 5 μ*M*) of ammonia were found which correspond with the highest measured atmospheric ammonia concentrations. There were higher standing stocks of phytoplankton, and higher primary production in the mixed layers of the ST and STCZ than in the polar and Subantarctic waters. Microzooplankton grazing rates were a little less than the phytoplankton growth rates, suggesting that in early to mid November grazing was controlling phytoplankton biomass. This spatial heterogeneity in primary production, and microzooplankton grazing may be responsible for the patterns in DMS and DMSP reported here and also by *Jones et al.* [1998] and *Bates et al.* [1998b].

It is unclear whether the higher primary production measured in the eastern block 10-12 days after sampling along the western transect is due to mesoscale patchiness or reflects the temporal progression of the spring bloom in these waters. The very high surface chlorophyll-*a* levels (up to 2.1 mg m^{-3}) in Subantarctic waters, found by the RV *Discoverer* during the Lagrangian B experiment in early December, suggest the spring bloom had finally begun. *Harris et al.* [1987] have shown that the onset of the spring bloom can occur at any time between September and January off Tasmania's east coast, and this is controlled primarily by the strength of the westerly winds. They also show that the onset of the spring bloom is delayed in El Nino years, and 1995 was an El Nino year. *Hainsworth et al.* [1998] note that the meteorological activity during the ACE 1 intensive period was characterized by frequent cold front activity, below average temperatures, and the region was windier than average. These conditions would act to delay the onset of the spring bloom, and thus reduced the production of DMS in the surface ocean during the ACE 1 intensive experiment.

Acknowledgments. This research is a contribution to the International Global Atmospheric Chemistry (IGAC) Core project of the International Geosphere-Biosphere Programme (IGBP) and is part of the IGAC Aerosol Characterization Experiments. Chris Rathbone (CSIRO Division of Marine Research) prepared the sea surface composite image, and Louise Bell applied the water mass boundaries and

day numbers on the image. F.B.G. extends his special thanks to Bronte Tilbrook, Pru Bonham, and Don McKenzie for stepping in and carrying the burden of being Chief Scientist (B. Tilbrook) on the cruise, and carrying out the primary production and grazing dilution work (P. Bonham and D. McKenzie) when F.B.G. was unable at the last minute to participate in the cruise.

References

Airey, D., and G. Sandars, Automated analysis of nutrients in seawater, *CSIRO Mar. Lab. Rep., 166*, 95 pp., 1987.

Allanson, B.R., R.C. Hart, and J.R.E. Lutjeharms, Observations on the nutrients, chlorophyll, and primary production of the Southern Ocean south of Africa, *S. Afr. J. Antarct. Res., 10/11*, 3-14, 1981.

Bates, T.S., R.P. Kiene, G.V. Wolfe, P.A. Matrai, F.P. Chavez, K.R. Buck, B.W. Blomquist, and R.L. Cuhel, The cycling of sulfur in surface seawater of the Northeast Pacific, *J. Geophys. Res., 99*, 7835-7843, 1994.

Bates, T.S., B.J. Huebert, J.L. Gras, F.B. Griffiths, and P.A. Durkee, The International Global Atmospheric Chemistry (IGAC) Project's First Aerosol Characterization Experiment (ACE 1): An overview, *J. Geophys. Res., 103*, 16,297-16,318, 1998a.

Bates, T.S. V.N. Kapustin, P.K. Quinn, D.S. Covert, D.J. Coffman, C. Mari, P.A. Durkee, W. DeBruyn, and E. Saltzman, Processes controlling the distribution of aerosol particles in the lower marine boundary layer during the First Aerosol Characterization Experiment (ACE 1), *J. Geophys. Res., 103*, 16,369-16,384, 1998b.

Bradford, J.M., and F.H. Chang, Standing stocks and productivity of phytoplankton off Westland, New Zealand, February 1982, *N. Z. J. Mar. Freshwater Res., 21*, 71-90, 1987.

Bradford-Grieve, J.M., F.H. Chang, M. Gall, S. Pickmere, and F. Richards, Size-fractionated primary phytoplankton standing stocks and primary production during austral winter and spring 1993 in the subtropical convergence region near New Zealand, *N. Z. J. Mar. Freshwater Res., 31*, 201-224, 1997.

Businger, S., J. Katzfey, R. Johnson, S. Siems, and Q. Wang, Smart tetroons for Lagrangian air mass tracking during ACE 1, *J. Geophys. Res., 104*, 11,709-11,722, 1999.

Clementson, L.A., J.S. Parslow, F.B. Griffiths, V.D. Lyne, D.J. Mackey, G.P. Harris, D.C. McKenzie, P.I. Bonham, C.A. Rathbone, and S. Rintoul. Controls on phytoplankton production in the Australian sector of the subtropical convergence. *Deep Sea Res., 45*, 1627-1661, 1998.

Cooper, D.J., and E.S. Saltzman, Measurements of atmospheric dimethylsulfide, hydrogen sulfide, and carbon disulfide during GTE/CITE 3, *J. Geophys. Res., 98*, 23,397-23,410, 1993.

CSIRO, Oceanographical observations in the Pacific Ocean in 1961, HMAS Gasgoyne Cruise G1/61. *CSIRO Div. Fish. and Oceanogr. (Aust.) Rep. No. 8*,1-136, 1963.

Curran, M.A.J., G.B. Jones, and H. Burton, Spatial distribution of dimethylsulfide and dimethylsulfoniopropionate in the Australian sector of the Southern Ocean, *J. Geophys., Res., 103*, 16,677-16,690, 1998.

Dacey, J.W.H., and S.G. Wakeham, Oceanic dimethylsulfide: Production during zooplankton grazing, *Science, 233*, 1314-1316, 1986.

Danckwerts, P.V., *Gas Liquid Reactions*, McGraw-Hill, New York, 1970.

De Bruyn, W.J., T.S. Bates, J.M. Cainey, and E.S. Saltzman., Shipboard measurements of dimethyl sulfide and SO_2 southwest of Tasmania during the First Aerosol Characterization Experiment (ACE 1), *J. Geophys. Res., 103*, 16,703–16,711, 1998.

Dickson, A.G., The measurement of sea water pH, *Mar. Chem., 44*, 131-142, 1993.

Downer, K.M., and M.I. Lucas, Photosynthesis-irradiance relationships and production associated with a warm-core ring shed from the Agulhas Retroflection south of Africa, *Mar. Ecol. Prog. Ser., 95*, 141-154, 1993.

Dring, M.J., and D.H. Jewson, What does ^{14}C uptake by phytoplankton really measure? A theoretical modeling approach, *Proc. R. Soc. London, Ser. B, 214*, 351-368, 1982.

Eppley, R.W., Temperature and phytoplankton growth in the sea, *Fish. Bull., U.S., 70*, 1063-1085, 1972.

Furuya, K., H. Hasumoto, T. Nakai, and T. Nemoto, Phytoplankton in the subtropical convergence during the austral summer: Community structure and growth activity, *Deep Sea Res., 33*, 621-630, 1986.

Genfa, Z., and P.K. Dasgupta, Fluorometric measurement of aqueous ammonium ion in a flow injection system, *Anal. Chem., 61*, 408-412, 1989.

Geider, R.J., Light and temperature dependence of the carbon to chlorophyll *a* ratio in microalgae and cyanobacteria: Implications for physiology and growth of phytoplankton, *New Phyto., 106*, 1-34, 1987.

Gibson, J.A.E., R.C. Garrick, H.R. Burton, and A.R. McTaggart, Dimethlysulfide and the alga *Phaeocystis pouchetii* in antarctic coastal waters, *Mar. Biol., 104*, 339-346, 1990.

Godfrey, J.S., D.J. Vaudrey, and S.D. Hahn, Observations of the shelf-edge current south of Australia, winter, 1982, *J. Phys. Oceanogr., 16*, 668-679, 1986.

Hainsworth, A.H.W., A.L. Dick, and J.L. Gras, Climatic context of the First Aerosol Characterization Experiment (ACE 1): A meteorological and chemical overview, *J. Geophys. Res., 103*, 16,319-16,340, 1998.

Hara, S., and E. Tanoue, Protist along 150°E in the Southern Ocean: Its composition, stock and distribution, *Trans. Tokyo Univ. Fish., 6*, 99-115, 1985.

Harris, G.P., C. Nilsson, L.A. Clementson, and D. Thomas, The water masses of the east coast of Tasmania: Seasonal and interannual variability and the influence on phytoplankton biomass and productivity, *Aust. J. Mar. Freshwater Res., 38*, 569-590, 1987.

Harris, G.P., F. B. Griffiths, L.A. Clementson, V. Lyne and H. van der Doe, Seasonal and interannual variability in physical processes, nutrient cycling, and the structure of the food chain in Tasmanian shelf waters, *J. Plankton Res., 13*, 109-131, 1991.

Harrison, W.G., Regeneration of nutrients, in *Primary Productivity and Biogeochemical Cycles in the Sea,* edited by P.G. Falkowski and A.D. Woodhead, pp. 385-407, Plenum, New York, 1992.

Holm-Hansen, O., S.Z. El-Sayed, G.A. Franceschini, and R L. Cuhel, Primary production and the factors controlling phytoplankton growth in the Southern Ocean, in *Adaptations Within Antarctic Ecosystems*, Proceedings of the 3rd SCAR Symposium on Antarctic Biology, edited by G.A. Llano, pp. 11-50, Smithsonian Institution, Washington, D.C.,1977.

Hosaka, N., and T. Nemoto, Size structure of phytoplankton carbon and primary production in the Southern Ocean south of Australia during the summer of 1983-84, *Mem. Natl. Inst. Polar Res. Spec. Issue, 40*, 15-24, 1986.

Hutchins, D.A., and K.W. Bruland, Iron-limited diatom growth and Si:N uptake ratios in a coastal upwelling regime, *Nature, 393*(6685), 561-564, 1998.

Jones, G.B., M.A.J. Curran, H.B. Swan, R.M. Greene, F.B. Griffiths, and L.A. Clementson, Influence of different water masses and biological activity on dimethylsulphide and dimethylsulfoniopropionate in the subantarctic zone of the Southern Ocean during ACE 1, *J. Geophys. Res., 103*, 16,691-16,702, 1998.

Jones, R. D., An improved fluorescence method for the determination of nanomolar concentrations of ammonium in natural waters, *Limnol. Oceanogr., 36*, 814-819, 1991.

Kamykowski, D., and S.J. Zentara, Circumpolar plant nutrient covariation in the Southern Ocean: Patterns and processes, *Mar. Ecol. Prog. Ser., 58*, 101-111, 1989.

Keller, M.D., W.K. Bellows, and R.R.L. Guillard, Dimethylsulfide production in marine phytoplankton, in: *Biogenic Sulfur in the Environment,* ACS Symp. Ser., vol. 393, edited by E.S. Saltzman and W.J. Cooper, pp 161-182, Am. Chem. Soc., Washington, D.C., 1989.

Kiene, R.P., and T.S. Bates, Biological removal of dimethylsulfide from seawater, *Nature, 345*, 702-705, 1990.

Landry, M.R., Estimating rates of growth and grazing mortality of phytoplankton by the dilution method, in *Handbook of Methods in Aquatic Microbial Ecology,* edited by P.F. Kemp et al., pp. 715-722, A.F. Lewis, New York, 1993.

Landry, M.R., and R.P. Hassett, Estimating the grazing impact of marine micro-zooplankton, *Mar. Biol., 67*, 283-288, 1983.

Laubscher, R.K., R. Perissinotto, and C.D. McQuaid, Phytoplankton production and biomass at frontal zones in the Atlantic sector of the Southern Ocean, *Polar Biol., 13*, 471-481, 1993.

Leck, C., U. Larsson, L.E. Bagander, S. Johanssen, and S. Hadja, DMS in the Baltic Sea: Annual variability in relation to biological activity, *J. Geophys. Res., 95*, 3353-3363, 1990.

Levasseur, M., S. Michaud, J. Egge, G. Cantin, J. C. Nejstgaard, R. Sanders, E. Fernandez, P. T. Solberg, B. Heimdal, and M. Gosselin, Production of DMSP and DMS during a mesocosm study of an *Emiliania huxleyi* bloom: Influence of bacteria and *Calanus finmarchicus* grazing, *Mar. Biol., 126*, 609-618, 1996.

Lewis, M.R., and J.C. Smith, A small volume, short-incubation-time method for measurement of photosynthesis as a function incident irradiance, *Mar. Ecol. Prog. Ser., 13*, 99-102, 1983.

Liss, P.S., and L. Merlivat, Air-sea gas exchange rates: Introduction and synthesis, in *The Role of Air-Sea Exchange in Geochemical Cycling*, edited by P. Buat-Menard, pp.113-127, D. Reidel, Norwell, Mass.,1986.

Liss, P.S., and P.G. Slater, Flux of gases across the air-sea interface, *Nature, 247*, 181-184, 1974.

Mackey, D.J., J. Parslow, H.W. Higgins, F.B. Griffiths, and J.E. O'Sullivan, Plankton productivity and biomass in the western equatorial Pacific: Biological and physical controls, *Deep Sea Res., 42*, 499-533, 1995.

Maeda, M., Y. Watanabe, N. Matsuura, D. Inagake, Y. Yamaguchi, and Y. Aruga, Surface distribution of nutrients in the Southern Ocean south of Australia, *Trans. Tokyo Univ. Fish., 6*, 23-42, 1985.

Malin, G., S. M. Turner, P. S. Liss, P. M. Holligan, and D. Harbour, Dimethylsulphide and dimethylsulphoniopropionate in the north-east Atlantic during the summer coccolithophore bloom, *Deep Sea Res., 40*, 1487-1508, 1993.

Mantoura, R.F.C., S.W. Jeffrey, C.A. Llewellyn, H. Claustre, and C.E. Morales, Comparison between spectrophotometric, fluorometric and HPLC methods for chlorophyll analysis. in *Phytoplankton Pigments in Oceanography,* edited by S.W Jeffrey, R.F.C. Mantoura, and S.W. Wright, pp. 361-380, Monogr. Oceanogr. Methodol. Vol. 10, U.N. Educ., Sci., and Cult. Org., Paris, 1997.

Marra, J., Analysis of diel variability in chlorophyll fluorescence, *J. Mar. Res., 55*, 767-784, 1997.

McCartney, M.S., Subantarctic mode water, in: A Voyage of Discovery, edited by M.V. Angel, pp. 103-119, Pergamon, Tarrytown, N.Y., 1977.

Minas, H.J., and M. Minas, Net community production in "High nutrient, low-chlorophyll" waters of the tropical and Antarctic Oceans: Grazing vs iron hypothesis, *Oceanol. Acta, 15*, 145-162, 1992.

Mitchell, B.G., and O. Holm-Hansen, Observations and modeling of the Antarctic phytoplankton crop in relation to mixing depth, *Deep Sea Res., 38*, 981-1007, 1991.

Morrow, R., J. Church, R. Coleman, D. Chelton, and N. White, Eddy momentum flux and its contribution to the Southern Ocean momentum balance, *Nature, 357*, 482-484, 1992.

Owens, W.B., and R.C. Millard, A new algorithm for CTD oxygen calibration, *J. Phys. Oceanogr., 15*, 621-631, 1985.

Parslow, J.S., J.A. Koslow, F.B. Griffiths, L. Clementson, C. Rathbone, P. Bonham, and D. McKenzie, Tasmanian slope trophodynamics, final report, 40 pp, Fish. Res. Dev. Counc., Hobart, Tasmania, Australia, 1996.

Parsons, T.R. and M. Takahashi, *Biological Oceanographic Processes*, Pergamon, Tarrytown, N.Y., 1975.

Parsons, T.R., Y. Maita, and C.M. Lalli, *A Manual of Chemical and Biological Methods for Seawater Analysis*, Pergamon, Tarrytown, N.Y., 1984.

Platt, T., C.L. Gallegos, and W.G. Harrison, Photoinhibition of photosynthesis in natural assemblages of marine phytoplankton, *J. Mar. Res., 38*, 687-701, 1980.

Quinn, P.K., and T.S. Bates, Collection efficiencies of a tandem sampling system for atmospheric aerosol particles and gaseous ammonia and sulfur dioxide, *Environ. Sci., Technol., 23*, 736-739, 1989.

Quinn, P.K., T.S. Bates, J.E. Johnson, D.S. Covert, and R.J. Charlson, Interactions between the sulfur and reduced nitrogen cycles over the central Pacific Ocean, *J. Geophys. Res., 95*, 16,405-16,416, 1990.

Quinn, P.K., D.J. Coffman, V.N. Kapustin, T.S. Bates, and D.S. Covert, Aerosol optical properties in the MBL during ACE 1 and the underlying chemical and physical aerosol properties, *J. Geophys. Res., 103*, 16,547-16,563, 1998.

Richards, F.A., Dissolved silicate and some related properties of some western N. Atlantic and Caribbean waters, *J. Mar. Res., 17*, 449-465, 1958.

Riemann, B., and L. M. Jensen, Measurements of phytoplankton primary production by means of the acidification and bubbling method, *J. Plankton Res., 13*, 853-862, 1991.

Rintoul, S.R., J.R. Donguy, and D.H. Roemmich, Seasonal evolution of upper ocean thermal structure between Tasmania and Antarctica, *Deep Sea Res., 44*, 1185-1202, 1997.

Sakshaug, E., A. Bricaud, Y. Dandonneau, P.G. Falkowski, D.A. Kiefer, L. Legendre, A. Morel, J. Parslow, and M. Takahasi, Parameters of photosynthesis: Definitions, theory, and interpretation of results, *J. Plankton Res., 19*, 1637-1670, 1997.

Sedwick, P.N., P.R. Edwards, D.J. Mackey, F.B. Griffiths, and J.S. Parslow, Iron and manganese in surface waters of the Australian subantarctic region, *Deep Sea Res., 44*, 1239-1253, 1997.

Stefels, J., and W.H.J. van Boekel, Production of DMS from dissolved DMSP in axenix cultures of the marine phytoplankton species *Phaeocystis* sp., *Mar. Ecol. Prog. Ser., 97*, 11-18, 1993.

Steidinger, K.A., and K. Tangen, Dinoflagellates, in *Identifying Marine Phytoplankton,* edited by C. R. Tomas, pp. 387-584, Academic, San Diego, Calif., 1997.

Stumm, W., and J.J. Morgan, *Aquatic Chemistry*, p. 109, John Wiley, New York, 1981.

Sullivan, C., K.R. Arrigo, C.R. McClain, J.C. Comiso, and J. Firestone, Distributions of phytoplankton blooms in the Southern Ocean, *Science, 262*, 1832-1837, 1993.

Sunda, W.G., and S. A. Huntsman, Interrelated influence of iron, light and cell size on marine phytoplankton growth, *Nature, 390*, 389-392, 1997.

Turner, S.M., G. Malin, P.S. Liss, D.S. Harbour, and P.M. Holligan, The seasonal variation of dimethylsulfoniopropionate concentrations in near-shore waters, *Limnol. Oceanogr., 33*, 364-375, 1988.

Vincent, W.F., G.C. Wake, P.C. Austin, and J.M. Bradford, Modeling the upper limit to oceanic phytoplankton production as a function of latitude in the New Zealand Exclusive Economic Zone, *N. Z. J. Mar. Freshwater Res., 23*, 401-410, 1989.

Whittlestone, S., and W. Zahorowski, Basclinc radon detectors for shipboard use: Development and deployment in the First Aerosol Characterization Experiment, *J. Geophys. Res., 103*, 16,743-16,751, 1998.

Wright, S.W., S.W. Jeffrey, R.F.C. Mantoura, C.A. Llewellyn, T. Bjornland, D. Repeta, and N. Welschmeyer, Improved HPLC method for the analysis of chlorophylls and carotenoids from marine phytoplankton, *Mar. Ecol. Prog. Ser., 77*, 183-196, 1991.

Yamamoto, T., Small-scale variations in phytoplankton standing stocks and productivity across the oceanic fronts in the Southern Ocean, *Mem. Natl. Inst. Polar. Res. Spec. Issue, 40*, 25-41, 1986.

T. S. Bates and P. K. Quinn, PMEL, NOAA, Seattle, WA 98115.
L. A. Clementson, F. B. Griffiths (corresponding author), and J. S. Parslow, CSIRO Marine Research, Castray Esplanade, Hobart, Tasmania 7000, Australia. (Brian.Griffiths@marine.csiro.au)

Received November 9, 1998; revised June 4, 1999;
accepted June 4, 1999.